Elucidation of antifibrotic effects for *Osbeckia octandra*: Isolation of main antifibrotic compounds and identification of regulatory molecular pathways

Osbeckia octandra の抗線維化効果の解析: 主要抗線維化化合物の同定とその調節経路の解明

The United Graduate School of Agricultural Science
Kagoshima University
Japan

Bogahawaththe Ralalage Sudarma Bogahawaththa

2023

Contents

Abbreviations

ALP: Alkaline phosphatase

ALT: Alanine transaminase

AST: Aspartate transaminase

ATF-6: Activating transcription factor 6

BiP: Binding immunoglobulin protein

BLE: Boiled leaf extract

BW: Body weight

CD44: cluster of differentiation 44

CLS: Crude leaf suspension

COL1A1: Collagen, type I, alpha 1

CON: Control

DW: Distilled water

ER: Endoplasmic reticulum

FeCl3: Iron (III) chloride

GRP78: 78 kDa glucose-regulated protein

H&E: Hematoxylin and eosin

HCC: Hepatocellular carcinoma

HLE: Hexane leaf extract

HPLC: High-performance liquid chromatography

HSCs: Hepatic stellate cells

HUVEC: human umbilical vein endothelial cells

IC_{50}: The half maximal inhibitory concentration

INT: Induced but not treated

IRE1-α: Inositol-requiring enzyme type 1alpha

MLE: Methanol leaf extract

mRNA: messenger ribonucleic acid

MT: Masson's trichrome

NMR: Nuclear magnetic resonance

PBS: Phosphate buffered saline

PERK: protein kinase R (PKR)-like endoplasmic reticulum kinase

ROS: Reactive oxygen species

ROS: Reactive oxygen species

SLE: Sonicated leaf extract

SMAD: Suppressor of mothers against decapentaplegic

TAA: Thioacetamide

TGF-β: Transforming growth factor-β

TLC: Thin-layer chromatography

TNF-α: Tumour necrosis factor-alpha

UPR: Unfolded protein response

UV: Ultraviolet

VEGF-R2*:* Vascular endothelial growth factor receptor-2

α–SMA: Smooth muscle alpha-actin

CHAPTER 01

General Introduction

Human liver is located in the upper right quadrant of the abdomen, below the diaphragm. The liver is a reddish brown wedge shaped organ with four lobes of unequal size and shape[1]. Lobules are the functional units of the liver. Each lobule is made up of millions of hepatic cells (hepatocytes) which are the basic metabolic cells. The lobules are held together by fine areola tissue. There are mainly two types of liver cells called parenchyma cells including parenchymal hepatocytes and non-parenchyma cells including hepatic stellate cells[1]. Human liver weighs about 1,500 g and accounts for 2.5% of the total body weight[2,3]. Liver is one of the most vital and largest organs in the human body that carries out various functions including metabolism, detoxification of various toxic insults, protein synthesis, production of clotting factors etc. Liver exposes many xenobiotics frequently, hence highly prone to many hepatic diseases. Once the liver is injured by any disease all its vital functions may get collapsed [3].

The liver can be damaged by a number of factors, including viral infections, alcohol abuse, fatty liver disease, medications, autoimmune diseases and genetic disorders. In the early stages of liver damage, there may be no obvious symptoms, but elevated liver enzymes in blood tests may indicate damage. At this stage, the liver may still be functioning relatively well. However, persistent damage triggers inflammation, which leads to the formation of scar tissue (fibrosis) in the liver. The progression of this liver fibrosis is a critical stage and it leads to more severe stages known as liver cirrhosis, where healthy liver tissue is replaced by non-functioning scar tissue and hepatocellular carcinoma (HCC) [4,5]. Cirrhosis significantly reduces liver function, resulting in symptoms such as jaundice, swelling, fatigue and an increased risk of complications. In the most severe cases, advanced cirrhosis can lead to liver failure. The World

Health Organization statistics, cirrhosis affects one percent of the world population, and HCC becomes to the fifth most common cause of cancer [6]. Liver fibrosis and cirrhosis also impose a considerable economic burden to society [7].

There are several potential drugs, such as doxorubicin [8], metformin [9] and silymarin [10], that have been shown to have antifibrotic effects, however, they have not been able to produce significant therapeutic effects in clinical practice. Liver transplantation is currently the only option for long-term survival in patients with liver disease. However, the procedure is expensive and finding a suitable donor is difficult. Considerable efforts are currently being devoted to research into liver fibrosis, not only with the goal of further understanding the molecular mechanisms that drive fibrosis but also with an equal in focus on establishing effective therapeutic strategies.

The art of curing of hepatic diseases through traditional medicine is prominent in many countries of the world, especially in Asian countries such as Sri Lanka, Thailand, India, China and Japan[11,12,13,14]. Therefore, when investigating new therapeutic strategies to cure liver fibrosis and cirrhosis, the preference is shifting to complementary and alternative medicines, which are either natural products or their derivatives [15]. The basis for this preference is their edibility which is generally accepted as having safe and long-lasting therapeutic potential [16]. As part of our ongoing projects to explore biologically active and unique natural products from herbal plants, we focused on *Osbeckia octandra*, which has been used as a traditional medicine in Sri Lanka for the treatment of jaundice caused by infection inducible and late stage liver diseases[17]. *O. octandra* is a highlighting plant in treatment of liver disorders (Figure 1.1). And also *O. octandra* leaves have become an important ingredient among Sri Lankan community in preparation of herbal porridges (Kola kanda)[18,19].

Previous pharmacological studies on *O. octandra* have shown that extracts of this plant have anti-oxidative, anti-inflammatory, and anti-cancer properties [20]. Several bioactive chemical

components, gallic acid, protocatechuic acid, kaempferol and quercetin have been isolated from another species of the same plant family, namely *Osbeckia aspera* [21]. However, the exact antifibrotic effects of these compounds remain poorly understood. As for *O. octandra*, no efforts have been made to isolate and identify any specific compounds from this species. Therefore, it is worthwhile to identify the antifibrotic compounds present in the crude extracts and their intervention in the pathways of fibrosis progression.

In this study, our first objective was to evaluate the prophylactic effect of different extracts and then select the best effective fraction for the further study. Next, therapeutic potential also investigated with the selected extract. We then isolated the key anti-fibrotic compounds using LX-2 cells, a fibrosis status screening model based on human-derived hepatic stellate cells (HSCs) and investigated their therapeutic interventions to ameliorate fibrosis. Taken together, these findings suggest that *O. octandra* can be used as a potential therapeutic agent for managing fibrosis status by mediating fibrosis progression pathways.

a

b

Figure 1.1: Plant of *Osbeckia octandra*. (a) This plant, commonly known as "Heen Bowitiya" in Sri Lanka, is a flowering plant that belongs to the Melastomataceae family. It is native to Sri Lanka and can be found growing in the wet zone of the country, especially in the central hills. The plant typically grows up to 2 meters in height and has a woody stem with branches that spread out horizontally. The plant produces small, pinkish-purple flowers that bloom in clusters at the ends of the branches. (b) The leaves are simple, opposite, and ovalshaped, with a glossy green color and smooth texture.

CHAPTER 02

Hepatoprotective effects of different leaf extracts of *Osbeckia octandra* on thioacetamide (TAA)-induced liver fibrosis in Wistar rats

2-1. Introduction

Liver fibrosis is a progressive disease characterised by the excessive accumulation of extracellular matrix proteins, leading to liver dysfunction and impaired liver architecture [22]. It is a significant global health problem associated with various chronic liver diseases such as cirrhosis and HCC [4,5]. Finding effective preventive measures and alternative therapies for liver fibrosis is of paramount importance. In recent years, the potential of natural products derived from medicinal plants has attracted considerable attention due to their therapeutic properties and minimal side effects [15]. Among these plants, *Osbeckia octandra*, a species found in tropical and subtropical regions, has been traditionally used to treat liver diseases. Previous pharmacological studies on *O. octandra* have shown that extracts of this plant have anti-oxidative, anti-inflammatory, and anti-cancer properties [20].

Understanding and harnessing the prophylactic effect in the context of liver fibrosis is crucial for several reasons. First, it allows early intervention, enabling healthcare professionals to detect and prevent the disease before it progresses, increasing the chances of successful prevention and preservation of liver function. Secondly, prophylaxis reduces the burden of advanced liver disease by slowing the progression of fibrosis, resulting in improved quality of life, reduced healthcare costs and lower mortality rates. In addition, prophylactic interventions often use natural products or less invasive measures, minimising the side effects of treatment. Furthermore, by emphasising the prophylactic effect in public health efforts, high-risk populations can be targeted and preventive strategies can be implemented to reduce the overall burden of liver disease. Finally, the holistic approach promoted by prophylactic interventions empowers individuals to take an active role in their own health and make informed choices to

reduce their risk of liver fibrosis and related conditions, thus promoting overall well-being and disease prevention.

To evaluate the prophylactic potential of *O. octandra*, thioacetamide (TAA) has been widely used to induce liver fibrosis in animal models. TAA mimics the progressive nature of human liver fibrosis and serves as a valuable tool for investigating preventive or therapeutic interventions. Given the traditional use of *O. octandra* in liver disease, it is crucial to investigate its prophylactic effects on TAA-induced liver fibrosis.Therefore, the aim of this study is to investigate the prophylactic effect of different leaf extracts of *O. octandra* on TAA-induced liver fibrosis in Wistar rats. By assessing biochemical markers, histological changes and antioxidant status, we can elucidate the mechanisms underlying the protective effect of *O. octandra* against liver fibrosis.

This chapter aim was to provide a comprehensive understanding of the prophylactic effect of different extract from *O. octandra*. First, assessed the biochemical markers related to liver fibrosis, such as liver enzymes and pro-inflammatory cytokines. Secondly, histological analysis were performed to assess the liver tissue architecture and fibrotic changes. The results of this study may shed light on the potential therapeutic applications of *O. octandra* in the prevention of liver fibrosis.

2-2. Experimental Section

2-2-1. Plant Materials

For the animal experiment, leaves of *O. octandra* were collected from the garden of the Department of Animal Science, Faculty of Agriculture, University of Peradeniya, Sri Lanka. The plant specimens were authenticated by the Curator of the Royal Botanical Gardens in Peradeniya, Sri Lanka, and a voucher specimen (*Osbeckia octandra* specimen No. UB 89) was deposited in the National Herbarium.

2-2-2. Leaf Extracts Preparation

Fresh *O. octandra* leaves (50 g) were washed with distilled water and air-dried at room temperature and freeze-dried using freeze drier, Alpha 1-4 LD plus (Christ, Osterode am Harz, Germany). The crude leaf suspension (CLS) was prepared by suspending freeze-dried leaf powder dissolved in 500 mg/mL of distilled water (DW) to prepare a stock solution. A total of 30 g of freeze-dried powder was mixed with 480 mL of distilled water and then boiled for boiled leaf extract (BLE), and the same mixture was sonicated in ultrasonic cleaner (VWR International, Randor, PA, USA) for 20 min to obtain sonicated leaf extract (SLE). A total of 30 g of freeze-dried powder, mixed with 480 mL of methanol or hexane and sonicated for 20 min, followed by filtration and solvent evaporation at 50 °C prior to overnight (37 °C) vacuum drying was used for methanol leaf extract (MLE) and hexane leaf extract (HLE). Prepared powder (BLE, SLE, MLE and HLE) (1 g) from each extract was dissolved in 500 mg/mL of DW to prepare a stock solution**.**

2-2-3. Experimental Animals

Six-week-old, male Wistar rats (220–240 g) were obtained from the Medical Research Institute, Borella, Sri Lanka. They were housed individually at the vivarium of the Faculty of Medicine, University of Peradeniya, Peradeniya, Sri Lanka under standard conditions (22 ± 3

°C with a 12 h light-dark cycle). The animals were fed with a standard commercial diet and provided tap water *ad libitum*. 30 rats were given an injection of thioacetamide (TAA) (Sigma, St. Louis, MO, USA) dissolved in physiological saline (154 mM NaCl) at a dose of 100 mg/kg body weight, intraperitoneally, twice a week, for 15 weeks to induce fibrosis. The TAA injecting rats were divided into six groups (n = 5 per group). The first group of rats who served as the TAA only treated group and orally gavaged twice weekly with DW (TAA only group). The remaining rats were orally gavaged twice weekly with CLS (500 mg/kg BW), BLE (500 mg/kg BW), SLE (500 mg/kg BW), MLE (500 mg/kg BW) and HLE (500 mg/kg BW). Leaf extracts and distilled water treatments were done simultaneously with TAA injection to investigate the protective effects of the different extracts. The doses used in this study were proven to be non-toxic. The remaining five rats were injected intraperitoneally with an equivalent volume of normal saline and orally gavaged with an equivalent volume of DW and served as the control group (CON). All rats were euthanized under isoflurane anesthesia in an induction chamber with isoflurane 3.5% for 2–5 min at 15 weeks after the treatments, and blood and liver samples were collected. Experimental procedures were carried out according to the institutional (Faculty ethic committee, Faculty of Veterinary Medicine and Animal Science, University of Peradeniya, Sri Lanka) animal ethics guidelines on the conduct of animal experimentation and animal care (Certificate No. VER-16-001). (Figure 2-1).

2-2-4. Body and liver weights assessment

The body weights of the rats were measured at the beginning of the study and the final body weights were measured before the animals were sacrificed. Liver weights were measured after sacrifice.

2-2-5. Serum collection and blood chemistry

Serum was separated from the collected blood and stored at -20°C. Samples were analyzed for alanine aminotransferase (ALT), aspartate aminotransferase (AST) and alkaline phosphatase

(ALP) using a 3000 Evolution (Biochemical Systems International, Arezzo, Italy) according to the manufacturer's instructions.

2-2-6. Tissue preparation and histopathology

Collected liver samples were fixed in 4% paraformaldehyde in phosphate buffered saline (PBS), embedded, and sectioned using a microtome and mounted on glass slides. Liver sections were stained with hematoxylin and eosin (H&E) for histopathology and masson's trichrome (MT) for collagen deposition [23].

2-2-7. RNA isolation and quantitative PCR

Total RNA from the mouse liver and the cells was extracted using Trizol (Thermofisher Scientific, Waltham, MA, USA) according to the manufacturer's instructions. The extracted RNA was then reverse transcribed using the cDNA Synthesis ReadyMix (Applied Biosystems, Foster City, CA, USA). The resulting cDNA was used as a template for quantitative PCR (qPCR) using the SYBER green real-time (Promega, Madison, WI, USA) using an ABI 7500 real time PCR platform (Applied Biosystems) according to the manufacturer's protocol. The primers used for this study are listed in Table 2-1. *α-Sma*, *Tgf-β1*, *Tnf-α* and *Vegf-R2* were amplified using 40 cycles with each cycle of denaturing at 95 °C for 15 sec followed by annealing and extension at 60 °C for 1 min and analysed using $2^{-\Delta\Delta CT}$ method using SDS 7000 software (Applied Biosystems). 18s rRNA expression was used as the internal control to normalize mRNA expression data.

2-2-8. Statistical analyses

Statistical analyses were performed using one-way analysis of variance (ANOVA) with a Dunnett's test. Data are expressed as mean ± standard error of the mean (SEM) or mean ± standard deviation (SD).

2-3. Results

2-3-1. *O. octandra* extracts prevented body weight loss and normalized liver weight

To induce continuous liver fibrosis, TAA multiple intraperitoneal injection (i.p.) strategy was used. The endpoint weight and weekly body weight gain were recorded. In comparison with CON, TAA showed significantly low body weight gain. Compared to rats in TAA, the rats in CLS, BLE and SLE groups showed significantly higher body weight gains. On the other hand, MLE and HLE did not show any treatment effects (Figure 2-2a). In the TAA group, liver indices showed a significantly higher liver/body weight percentage compared to the CON. The liver indices of CLS, BLE and SLE treatments showed significantly lower values compared to that of TAA rats (Figure 2-2b). Interestingly, CLS, BLE and SLE treatments appear to have the potential to ameliorate TAA-induced liver damage.

2-3-2. *O. octandra* extracts restored serum concentrations of liver enzymes

To test liver functions, the serum alanine aminotransferase (ALT), aspartate aminotransferase (AST) and alkaline phosphatase (ALP) levels were measured at the end of the treatment period. The TAA group showed significantly higher ALT, AST and ALP values compared to CON. In comparison to the TAA, significantly low serum concentrations of ALT, AST and ALP were observed in the CLS and, BLE and SLE groups. (Figure 2-3a–c). The findings confirm the hepatocellular damage in TAA as evident by significantly higher enzyme levels. Treatments of CLS, BLE and SLE have shown protection against TAA-induced hepatotoxicity by decreasing intracellular enzyme leakage.

2-3-3 *O. octandra* extracts restored gross liver appearance

The appearance (gross anatomy) of the liver surface was observed, and images were taken at the end of the experiment period to confirm the disease induction and treatment effects of the different leaf extracts of *O. octandra*. CON livers showed a normal liver appearance with a

smooth and shiny surface (Figure 2-4a). Prominent hepatic nodules of variable sizes were seen on the livers of TAA (Figure 2-4b). The CLS treated livers showed smooth surfaces similar to the CON (Figure 2-4c), while the BLE (Figure 2-4d) and SLE (Figure 2-4e) treated livers showed mild irregularity of the surface, although there were no prominent nodules. The livers of MLE (Figure 2-4f) and HLE (Figure 2-4g) groups showed prominent nodules with variable sizes similar to TAA (Figure 2-4b). Liver surface appearance changes in CLS, BLE and SLE treatments indicated mild improvements. The appearances further confirmed the recovery and possible protective effect of the extracts. Nevertheless, MLE and HLE did not show any favorable improvement.

2-3-4 *O. octandra* extracts restore liver architecture

We further examined the histopathological changes by staining the liver sections with hematoxylin and eosin (HE) and with Masson's trichrome (MT) for collagen deposition, and micrographs were captured under the light microscope. CON livers showed normal hepatic architecture (Figures 2-5a & Figures 2-6a). The livers from TAA showed regenerating hepatocytic nodules with complete fibrous bridges in hepatic parenchyma (Figures 2-5b & Figures 2-6b). The CLS treated livers showed mild fibrosis around the centrilobular region livers (Figures 2-5c & Figures 2-6c). Further, incomplete fibrous bridge formation (Figures 2-6d & Figures 2-6d) was observed in the livers of BLE, while complete fibrous bridge formation with regenerating hepatocytic nodules was observed in SLE (Figures 2-5e & Figures 2-6e), MLE (Figures 2-5f & Figures 2-6f) and HLE (Figures 2-5g & Figures 2-6g) treatment receiving rats. The data confirm the establishment of cirrhosis in TAA since complete fibrous bridges and hepatocytic nodules were very prominent under the TAA challenge. CLS and BLE treatments showed possible curative effects against the TAA-induced liver cirrhosis. However, complete fibrous bridges and nodule formation could still be seen in SLE, MLE and HLE treated liver sections, which may be due to mild or no beneficial effects.

2-3-5. *O. octandra* extracts ameliorate liver fibrosis

The collagen deposition of MT-stained liver sections was analyzed by Image J software. The liver fibrosis was significantly increased in TAA compared to that in the CON livers**.** However, the treatment of CLS, BLE and SLE extracts indicated a significant reduction of collagen deposition compared to TAA. Collagen deposition in MLE and HLE treatments was not reduced and was similar to TAA (Figure 2-7). These results further show possible hepatoprotective effects previously identified in aqueous extracts (CLS, BLE and SLE) but not in MLE and HLE.

2-3-6. *O. octandra* extracts prevent up-regulation of pro-inflammatory and profibrotic cytokine

To further confirm the disease establishment and the effects of different leaf extract, relative mRNA expressions of tumor necrosis factor-alpha (*Tnf-α*), alpha-smooth muscle actin (*α-Sma*), transforming growth factor-beta 1 (*Tgf-β*) and vascular endothelial growth factor 2 (*Vegf-R2*) were measured. As shown in Figure 2-8, in comparison to the CON (set as 1.0), significantly higher levels of *Tnf-α*, *α-Sma*, *Tgf-β* and *Vegf-R2*) mRNA expressions were observed in TAA. *Tnf-α* expression level was significantly lower in CLS, BLE and SLE in comparison to TAA (Figure 2-8a). Moreover, *α-Sma* mRNA expression level in CLS, BLE and SLE treated livers was significantly lower than the TAA (Figure 2-8b). *Tgf-β* mRNA expression level in CLS, BLE and SLE were significantly lower than TAA (Figure 2-8c). In addition, *Vegf-R2* mRNA expression levels in CLS and BLE were significantly lower than TAA and in SLE, livers did not show a significant difference compared to TAA (Figure 2-8d). The data confirmed the establishment of cirrhosis in TAA within 15 weeks by significantly increased mRNA expression levels of the identified markers. Significantly reduced expression levels were observed for pro-inflammatory and fibrotic cytokines expressions in CLS, BLE and SLE

further confirmed the hepatoprotection against TAA-induced liver cirrhosis at the molecular level as well.

2-3-7. *O. octandra* extract prevents angiogenesis

The *Vegf-R2* mRNA expressions in CLS and BLE treated rat livers suggested a potent anti-angiogenesis effect. Thus, to further study the effect, a standard in vitro angiogenic assay using human umbilical vein endothelial cells (HUVEC) seeded on a Matrigel model was used. The attachment of the cells occurred in the first hour and then followed by their migration towards each other over the next 2–4 h, forming capillary-like tubes, which matured by 6–16 h. In the control group, the cells were attached, aligned and formed tubes with a lumen that appears as a network (Figure 2-9a). The addition of BLE to the HUVEC medium significantly inhibited the formation of vessel-like structures and resulted in the cells remaining separated and somewhat rounded as solitary cells (Figure 2-9a). The HUVEC sprouting was significantly less pronounced with the addition of increasing concentrations of BLE. Furthermore, the number of branch points and tube length was significantly reduced with BLE treatment compared to that of the control (Figures 2-9b & c). These observations further confirm the anti-angiogenesis effect that was more potent in BLE.

2-4. Discussion

Liver fibrosis is a condition characterized by the excessive accumulation of scar tissue in the liver. It occurs because of chronic liver injury and inflammation [24]. When the liver is continuously injured, normally dormant hepatic stellate cells become activated and produce excessive amounts of extracellular matrix proteins such as collagen. This accumulation of scar tissue disrupts the normal structure of the liver and impairs its function. Several rat models are commonly used in research studies to induce liver fibrosis [25]. One of the most widely used methods is the administration of hepatotoxins, such as carbon tetrachloride (CCl_4) or thioacetamide (TAA), to induce liver injury and subsequent fibrosis [26]. These models closely mimic the progressive nature of human liver fibrosis and allow the investigation of the underlying mechanisms and potential therapeutic interventions.

In this study, we used TAA, a widely used hepatotoxin that mimics the progressive nature of human liver fibrosis. TAA induction triggers a series of cellular events, including inflammation, oxidative stress and activation of hepatic stellate cells, ultimately leading to the development of fibrotic scar tissue. For TAA-induced hepatic fibrosis in rats, the hepatotoxin is typically administered either by intraperitoneal injection or by inclusion in the drinking water or diet. TAA is metabolized in the liver, leading to the formation of reactive metabolites that induce oxidative stress, hepatocellular injury, inflammation and activation of hepatic stellate cells. TAA is mainly metabolized in the liver by hepatic microsomal enzymes, in particular the cytochrome P450 system. The metabolism of TAA involves several enzymatic reactions. Initially, TAA undergoes oxidative sulphuration mediated by cytochrome P450 enzymes, primarily CYP2E1, resulting in the formation of thioacetamide *S*-oxide (TASO). TASO can undergo further oxidative sulfoxidation mediated by flavin-containing monooxygenases (FMOs) or cytochrome P450 enzymes, resulting in the formation of thioacetamide *S*-dioxide (TASO2). Both TASO and TASO2 are reactive metabolites that can cause hepatotoxicity.

These reactive metabolites can bind to cellular macromolecules, induce oxidative stress and trigger inflammatory responses, leading to hepatocellular injury and the initiation of liver fibrosis [27].

In this study, we aimed to investigate the prophylactic effect of different extracts of *O. octandra* on liver fibrosis. We administered different extracts, including CLS, BLE, SLE, MLE and HLE, to rats and observed their effects on gross liver pathology. The results showed that CLS, BLE and SLE extracts exhibited hepatoprotective properties, as they normalized body weight, liver indices and the liver appearance of the treated rats. To further analyze the liver samples, were examined the release of the liver enzymes ALT, AST and ALP, which indicate chronic liver damage. The rats injected with TAA showed markedly elevated enzyme profiles, indicating liver damage, but treatment with CLS, BLE and SLE extracts reduced these enzyme levels. Histological examination showed that hepatocytes from CLS and BLE treated livers had a near-normal cellular architecture, supporting the improved biochemical data. This indicated that CLS and BLE extracts had the most potent hepatoprotective properties, probably due to the presence of active compounds in the extracts.

In cases of liver injury, inflammation and fibrogenesis play crucial roles. The study found that TAA i.p. injected rats showed increased gene expression of proinflammatory cytokines like TNF-α and activated HSCs, which secrete extracellular matrix (ECM), leading to liver fibrosis [28]. However, treatment with CLS, BLE, and SLE extracts inhibited the upregulation of *Tnf-α*, *α-Sma* (marker of activated HSCs), and *Tgf-β* (a key profibrotic cytokine) [28]. This indicated that these plant extracts efficiently suppressed the secretion of proinflammatory and profibrotic cytokines and inhibited HSCs activation, resulting in a reduction in liver fibrosis .

Recent data have highlighted the role of angiogenesis in the progression of fibrosis to cirrhosis [29]. In this study, the researchers investigated the angiogenic effect of BLE extract, as CLS

couldn't be used to treat cells due to its particulate nature. They used a tube formation assay, which includes endothelial cell adhesion, migration, protease activity and tube formation, to assess angiogenesis-related factors [30]. The results showed that BLE inhibited both branching and tube elongation in a dose-dependent manner, with the highest dose producing maximal inhibition.

In conclusion, the study demonstrated that BLE have significant hepatoprotective and antifibrotic effects, inhibiting inflammation and fibrosis in the liver. These findings suggest that BLE may be a promising candidate for the development of novel therapeutic anti-fibrotic agents for the treatment of patients with chronic liver disease. However, further investigation is required to identify the specific compounds responsible for these effects and to explore their potential as therapeutic options for liver disease. These findings open new avenues for the development of alternative treatments for liver fibrosis and cirrhosis.

Table 2-1: Primers used for qPCR in this chapter

Gene	Sequence
Rat-Tnf-α	F; 5′–GGCTGCCCCGACTATGTG–3′ R; 5′–CTCCTGGTATGAAGTGGCAAATC–3′
Rat-Tgf-β1	F; 5′–GAGGTGACCTGGGCACCAT–3′ R; 5′–GGCCATGAGGAGCAGGAA–3′
Rat-α-Sma	F; 5′–GACCCTGAAGTATCCGATAGAACA–3′ R; 5′–CACGCGAAGCTCGTTATAGAAG–3′
Rat-Vegf-R2	F; 5′–CTGCCTACCTCACCTGTTTCC–3′ R; 5′–CGGCTCTTTCGCTTACTGTTC–3′
Rat-18S	F; 5′–GTAACCCGTTGAACCCCATT–3′ R; 5′–CCATCCAATCGGTAGTAGCG–3′

[a] F; forward primer. [b] R; Reverse primer.

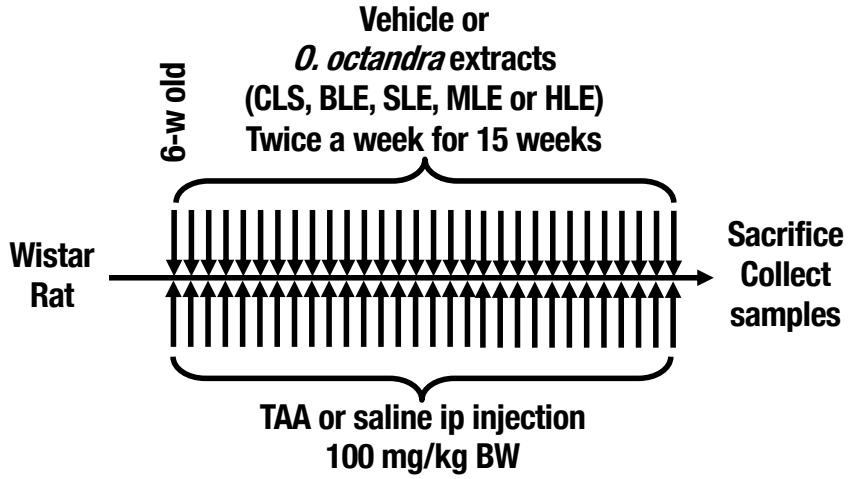

Figure 2-1: Experimental procedure. Wister rats were given an injection of TAA dissolved in a dose of 100 mg/kg body weight, intraperitoneally, twice a week, for 15 weeks to induce fibrosis. The TAA injected rats were divided into 6 groups. The first group of rats who served as the TAA only treated group and orally gavaged twice weekly with distilled water (DW). The remaining rats were orally gavaged twice weekly with CLS, BLE, SLE, MLE and HLE (500 mg/kg BW). Leaf extracts and DW treatments were done simultaneously with TAA injection to investigate the protective effects of the different extracts. The remaining five rats were injected intraperitoneally with an equivalent volume of normal saline and orally gavaged with an equivalent volume of DW and served as the control group (CON).

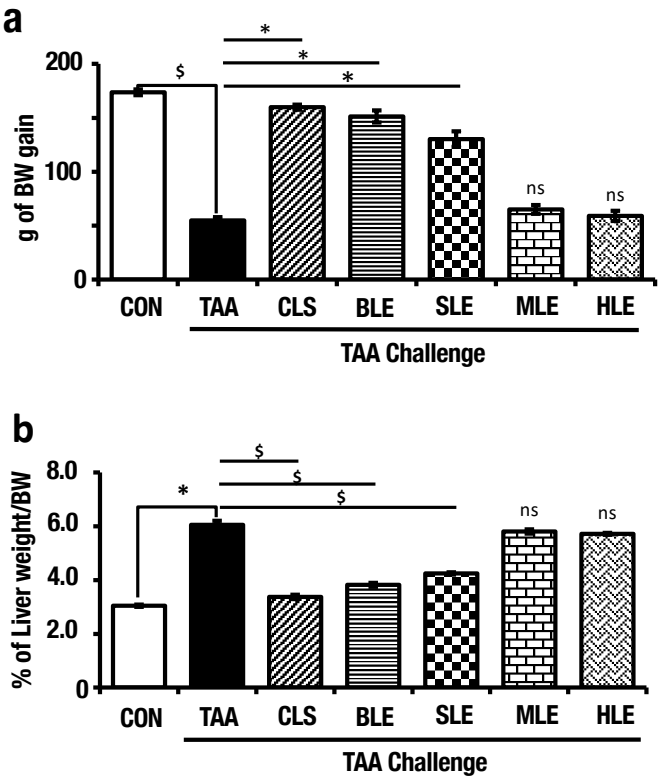

Figure 2-2: Aqueous extracts from *O. octandra* prevents body and liver weight retardation during the TAA challenge. (a) Body weight gain from the beginning to the end from each of the seven groups of rats (CON, TAA, CLS, BLE, SLE, MLE or HLE treatment model) during the TAA challenge. The values are indicated in grams of increase/decrease using the starting weight. (**b**) Liver/body weight ratio at the end from each of the seven groups of rats. Error bars represent standard errors of the means (SEM) in each group (n = 5). The statistical significance has been indicated in two ways; i) disease induction effect during the TAA challenge (CON vs. TAA), ii) *O. octandra* treatment consequence (TAA vs. CLS, BLE, SLE, MLE and HLE), with one-way ANOVA followed by the Dunnett's test. $, significant decrease; $, p = 0.05 to 0.01. *, significant increase; *, p = 0.05 to 0.01. ns, $p > 0.05$.

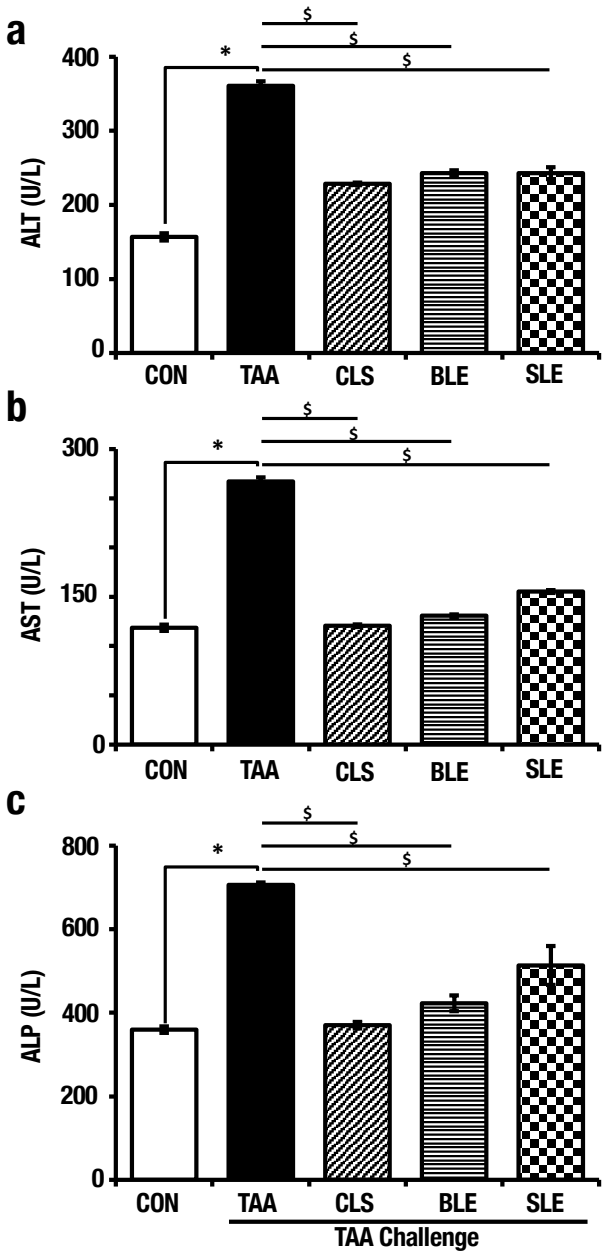

Figure 2-3: Selected aqueous extracts (CLS, BLE and SLE) protect the liver from TAA-induced damage by reducing the leakage of liver enzymes at the end of the treatment period. (a) Serum ALT levels, (**b**) serum AST levels and (**c**) serum ALP levels of CON, TAA and after treatments of aqueous extracts along with TAA challenge. Error bars represent standard errors of the mean (SEM) in each group (n = 5). The statistical significance of results has been shown in two ways; i) disease induction effect during the TAA challenge (CON vs. TAA), ii) *O. octandra* treatment effect (TAA vs. CLS, BLE and SLE) was analyzed with one-way ANOVA followed by the Dunnett's test. $, significant decrease; $, p = 0.05 to 0.01. *, significant increase; *, p = 0.05 to 0.01.

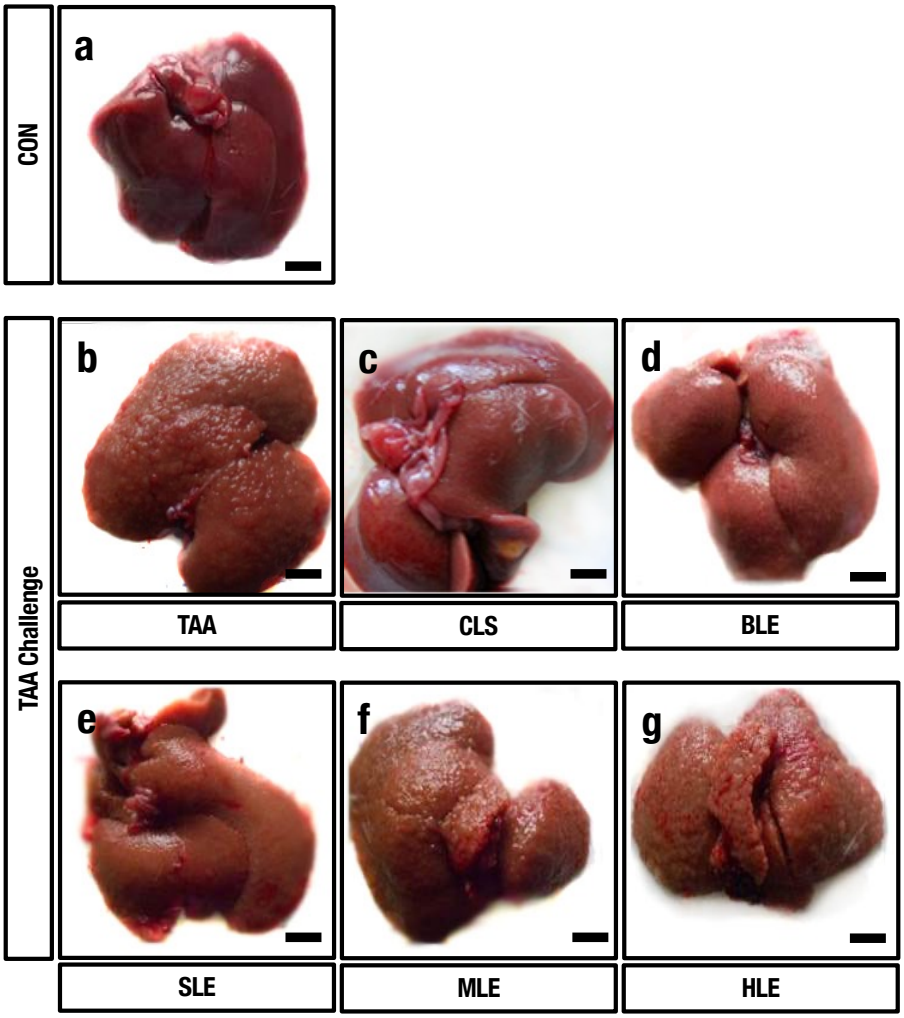

Figure 2-4: Aqueous extracts (CLS, BLE and SLE) demonstrated more potency to protect the liver against TAA challenge. (**a**) CON livers showed a normal appearance with a smooth surface. (**b**) Numerous nodules of various sizes can be seen on the liver surface of TAA. (**c**) Livers treated with CLS showed a smooth surface. (**d**) Small nodules can be seen on the surfaces of livers treated with BLE and (**e**) SLE. (**f**,**g**) Nodules of variable sizes were present on the surfaces of livers treated with MLE and HLE. Bar = 10 mm.

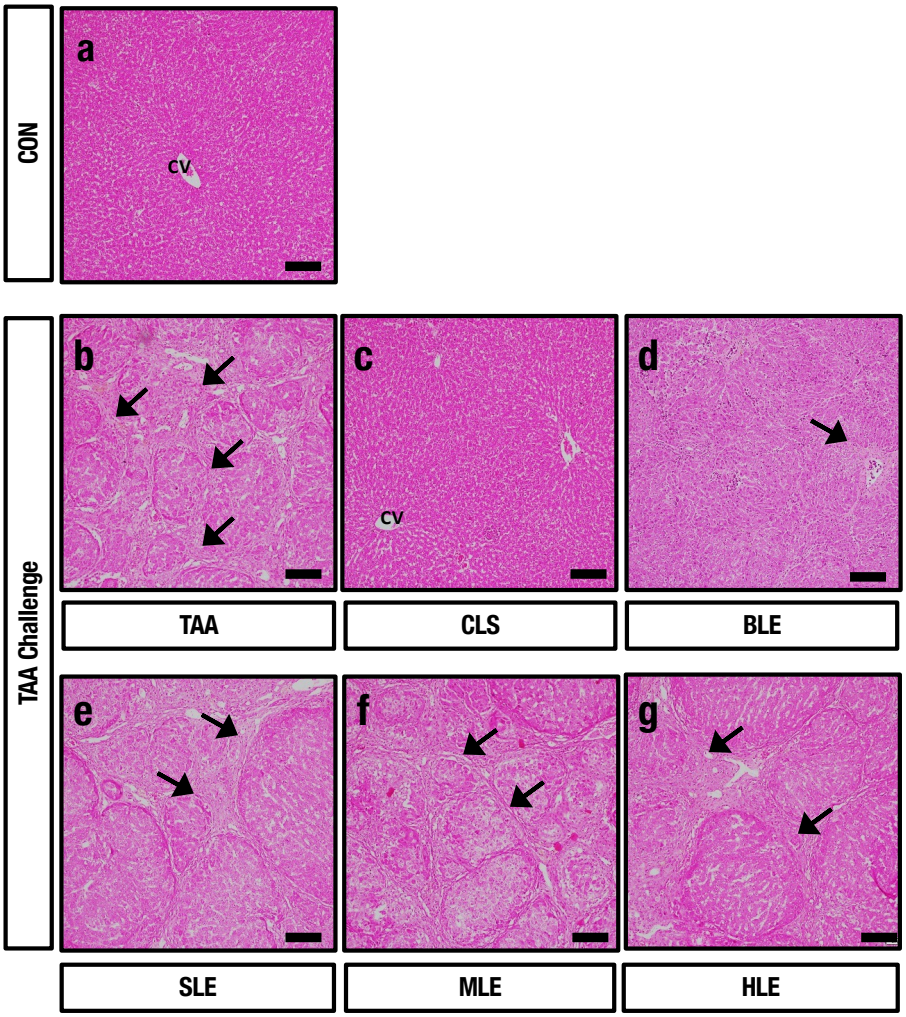

Figure 2-5: Hepatoprotective effect of aqueous extracts (CLS and BLE) against TAA-induced liver cirrhosis. Histopathological sections of livers (stained with HE) from CON, TAA and different leaf extract treatments of *O. octandra* CLS, BLE and SLE) after 15 weeks. (**a**) CON livers showed normal hepatic architecture and without histopathological changes. (**b**) Regenerating hepatic nodules formed by complete fibrous bridges were seen in the livers of TAA. (**c**) Animals treated with CLS showed normal hepatic architecture. (**d**) Incomplete fibrous bridge formation was seen in the animals treated with BLE. (**e**–**g**) Complete fibrous bridge formation with regenerating hepatocytes was observed in animals treated with SLE, MLE and HLE, respectively. CV, central vein. Bar = 100 µm.

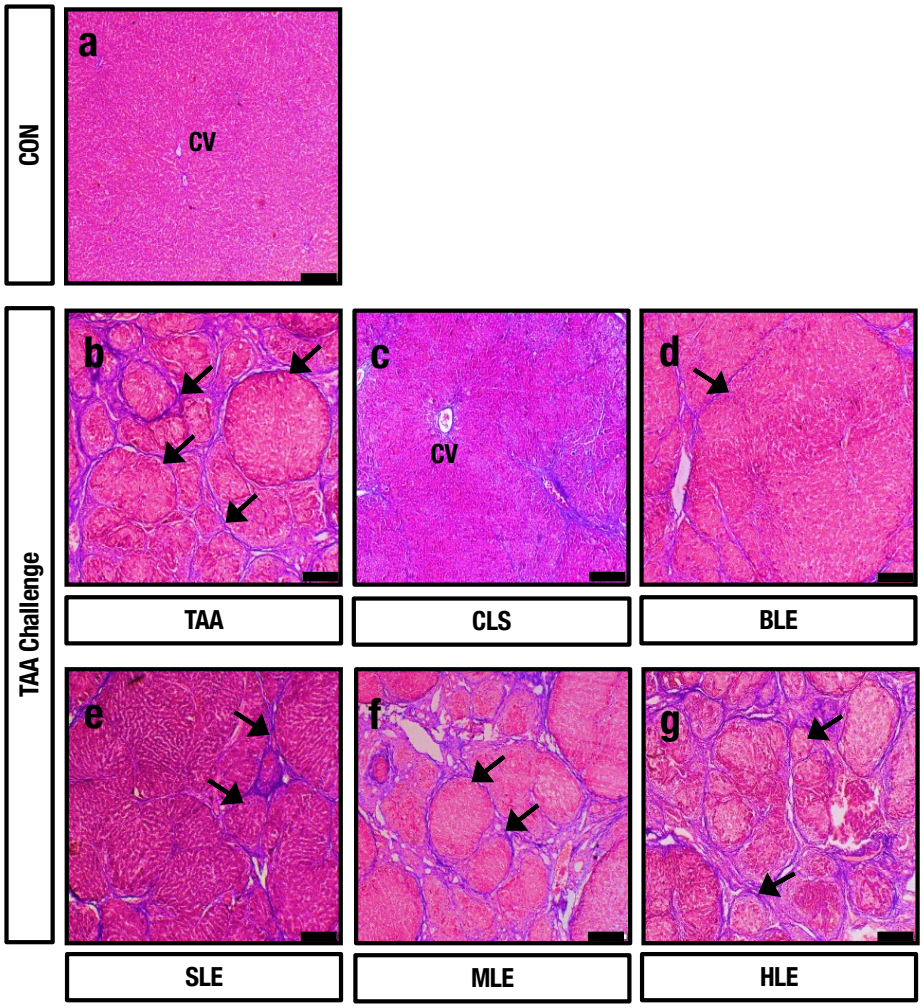

Figure 2-6: Aqueous extracts (CLS and BLE) showed an anti-fibrotic effect against TAA-induced liver cirrhosis. Histopathology of (stained with Masson's trichrome) CON, TAA and different leaf extracts of *O. octandra* treated CLS, BLE and SLE) livers at 15 weeks. (**a**) In the CON livers, collagen fibers were mainly seen in the vascular wall. (**b**) Increased collagen deposition in the thickened fibrous bridges was seen in TAA. (**c**) A small amount of collagen was detected mainly in the periportal and centrilobular areas in livers treated with CLS. (**d**) Livers treated with BLE showed a few collagen deposits as thin fibrous bridges. (**e**–**g**) Increased amounts of collagen with thickened fibrous bridges were observed in livers treated with SLE, MLE and HLE. CV, central vein. Arrows indicate collagen depositions. Bar = 100 μm.

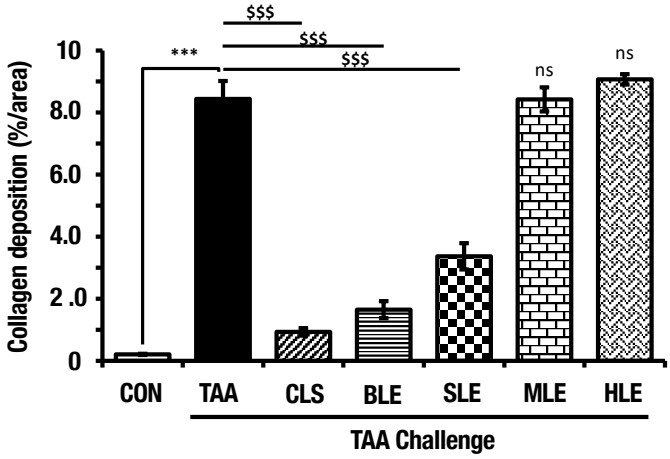

Figure 2-7: Treatments with aqueous extracts (CLS, BLE and SLE) showed a minimum amount of collagen deposits, indicating their hepatoprotective activity in TAA-induced liver cirrhosis. MT-stained liver sections were quantified using image J software. The values are indicated as percentages of the total surface. Error bars represent standard errors of the means (SEM) in each group (n = 5). The statistical significances are shown in two ways; i) disease induction effect during the TAA challenge (CON vs. TAA), ii) *O. octandra* treatment consequence (TAA vs. CLS, BLE, SLE, MLE and HLE), with one-way ANOVA followed by the Dunnett's test. $, significant decrease; $$$, $p < 0.001$. *, significant increase; ***, $p < 0.001$. ns, $p > 0.05$.

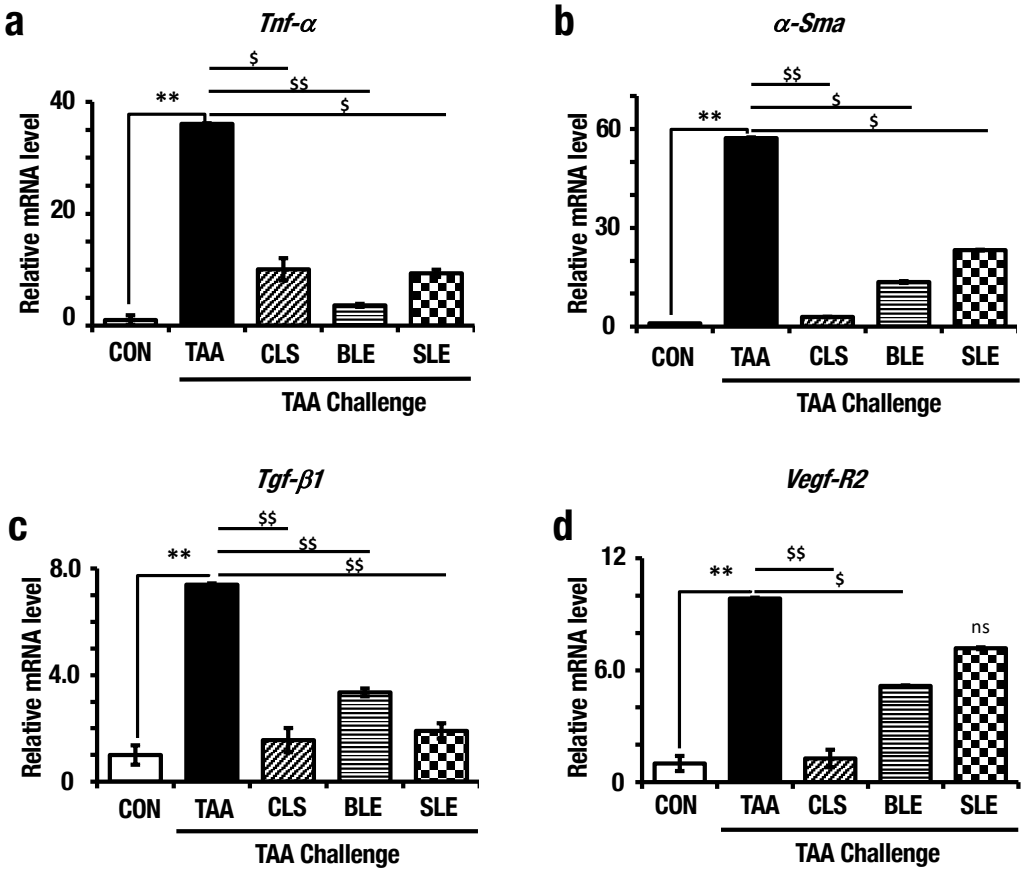

Figure 2-8: mRNA expressions confirmed the establishment of liver cirrhosis in TAA group and the hepatoprotective effect of aqueous extracts in the other treatments. (a) *Tnf-α*, (b) *α-Sma*, (c) *Tgf-β* and (d) *Vegf-R2* mRNA expressions determined by qPCR. Expression levels are normalized to *18S* mRNA level. Error bars represent standard errors of the means (SEM) in each group (n = 5). The statistical significances are indicated in two ways; i) disease induction effect during the TAA challenge (CON vs. TAA), ii) *O. octandra* treatment consequence (TAA vs. CLS, BLE and SLE), with one-way ANOVA followed by the Dunnett's test. $, significant decrease; $, p = 0.01 to 0.05, $$, p = 0.001 to 0.01, *, significant increase; **, p = 0.001 to 0.01. ns, $p > 0.05$.

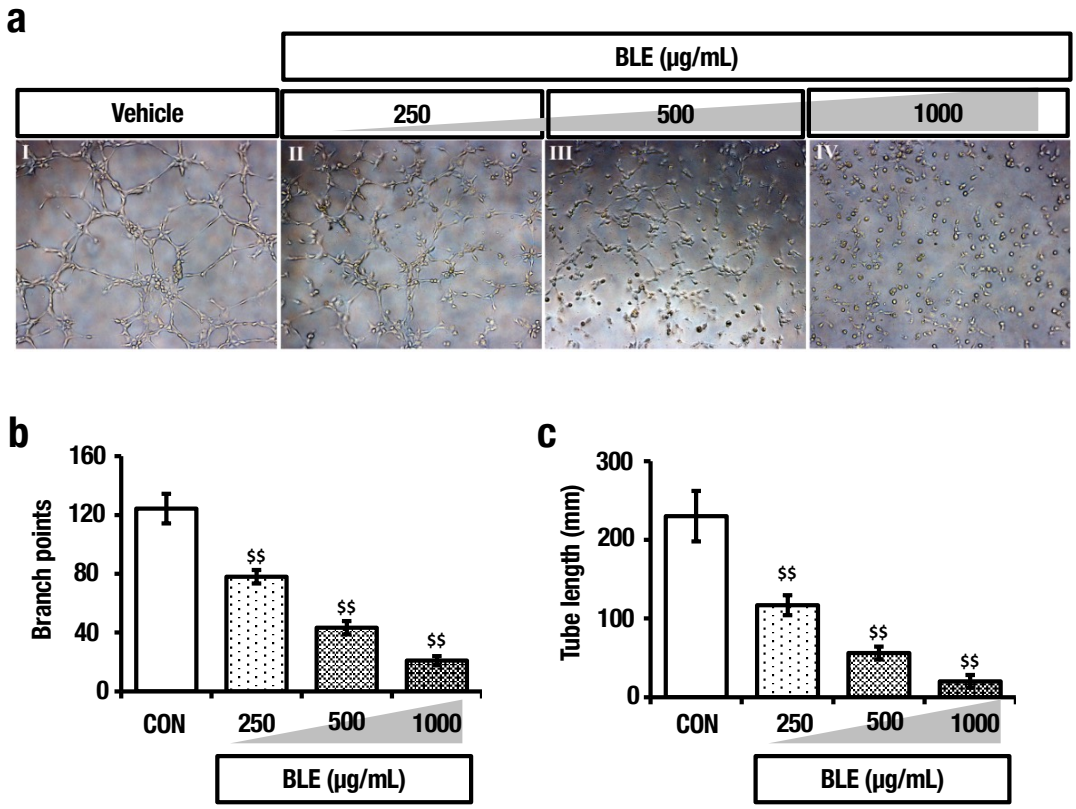

Figure 2-9: Boiled leaf extract (BLE) of *O. octandra* inhibited angiogenesis in the HUVEC model. (a) Representative micrographs of 4 h post-seeding. (I) HUVECS were attached, aligned and organized in tubes with a lumen that appeared as a network when cultured on ECM. (II–IV) In the presence of *O. octandra* extract, HUVECs were attached but remained somewhat rounded as solitary cells. The effect of *O. octandra* was dose-dependent, and when the concentration increased from 250 to 1,000 µg/mL, branching and tube formation was significantly inhibited. (b) Cumulative tube length and (c) number of branch points of capillary-like structures were also significantly reduced at 4 h. Error bars represent the standard error of the means (SEM) in each group (n = 3). The statistical significance was calculated with one-way ANOVA followed by Dunnett's test. $, significant decrease; $$, p = 0.001 to 0.01. ns, $p > 0.05$

CHAPTER 03

Therapeutic effect of different extracts of *Osbeckia octandra* on thioacetamide (TAA)-induced liver cirrhosis in Wistar rats

3-1. Introduction

In the previous chapter, we conducted a series of experiments to explore the potential benefits of the aqueous extract of *O. octandra* in recovering the antifibrosis effect in a rat model induced by TAA. This experiment served as a therapeutic study, aiming to cure fibrosis after occurring. However, it is equally important to investigate the therapeutic potential of selected extract (BLE) in addition to the CLS. Therapeutic effects hold significant importance, considering the increasing number of patients suffering from existing conditions such as fatty liver fibrosis and cirrhosis.

In this chapter, our primary objective was to evaluate the therapeutic potential of the selected extract, along with the crude leaf suspension. We aimed to delve deeper into understanding the effects of these treatments on pre-existing fibrosis. Our research aimed to provide valuable insights into the possibility of using these treatments as therapeutic interventions for patients already affected by these conditions.

The therapeutic effects of these treatments were then evaluated through a well-established animal model, which closely mimicked the conditions observed in human patients. Further analysis and validation are warranted to fully establish their efficacy and safety profiles. Nonetheless, this research paves the way for potential breakthroughs in the clinical management of patients affected by these conditions, offering new hope and possibilities for enhanced treatment strategies.

3-2. Experimental section

3-2-1. Plant materials and leaf extracts preparation

CLS and BLE was prepared as described previous chapter.

3-2-2. Experimental Animals

Six-week-old, male Wistar rats (220 - 240 g) were housed at the vivarium of the Faculty of Medicine, University of Peradeniya, Sri Lanka, and reared under the standard conditions (22 ± 3ºC with a 12-hour light-dark cycle). Ten rats were randomly assigned as the normal control group and 20 rats were injected with TAA (Merck) dissolved in physiological saline at a dose of 100 mg/kg BW, intraperitoneally, twice a week, for 5 weeks to induce fibrosis. Five rats from the control group 1 (CON1) and 5 rats from the TAA induced group (TAA) were sacrificed at the end of 5 weeks. The remaining 5 rats of the initial control group were kept as the control group 2 (CON2) and the remaining 15 rats of the TAA treated group were divided into 3 groups for the next 5 weeks of the study. Induced not treated group (INT) was given DW after the week 5. They were kept observing the natural regeneration of hepatocytes after chronic liver damage. The CLS only group was received CLS (500 mg/kg BW, orally, twice a week) and the BLE only group received BLE (500 mg/kg BW, orally, twice a week). All rats were euthanized under isoflurane anesthesia 10 weeks after the commencement of treatments and blood and liver samples were collected for analysis. Experimental procedures were conducted in accordance with the Institutional (Faculty ethic committee, Faculty of Veterinary Medicine and Animal Science, University of Peradeniya, Sri Lanka) Animal Ethics Guidelines for the conduct of Animal Experiments and Animal Care (Certificate No. VER-16-001). (Figure 3-1).

3-2-3. Body weight assessment

As described previous chapter

3-2-4. Serum collection and blood chemistry

As described previous chapter

3-2-6. Liver Weight Assessment

As described previous chapter

3-2-7. Tissue Preparation and Histopathology

As described previous chapter

3-2-8. RNA Extraction and Real-time Quantitative Polymerase Chain Reaction (qPCR)

Total RNA was extracted from liver samples using the Trizol method [31]. RNA (2 μg) was reverse-transcribed by using kit following the manufacturer's protocol (Applied Biosystems, USA) and qPCR was performed with SYBR green real-time PCR master mix (Promega, Madison, WI) using an ABI 7500 real time PCR platform according to the manufacturer's protocol (Applied Biosystems). *α-Sma*, *Tgf-β*, and *Tnf-α* and were amplified using 40 cycles with each cycle of denaturing at 95 °C for 15 sec followed by annealing and extension at 60 °C for 1 min and analysed using $2^{-\Delta\Delta CT}$ method with SDS 7000 software (Applied Biosystems). The primers used for this study are listed in Table 2-1 (chapter 2). 18S mRNA expression was used as the internal control to normalize mRNA expression data.

3-2-9. Statistical Analysis

Statistical analyses were performed using one-way analysis of variance (ANOVA) with a Dunnett's test. Data are expressed as mean ± standard error of the mean (SEM) or mean ± standard deviation (SD).

3-3. Results

3-3-1. Therapeutic effect of *O. octandra* leaf extracts in TAA-induced liver fibrosis

To evaluate the therapeutic effect, first fibrosis was induced by intraperitoneal (i.p.) injection of TAA for 5 weeks in a rat model as described in Figure 3-1. In this study, TAA-induced liver injury was assessed by gross-pathology, histopathology and immunohistochemistry. At the end of the week 5, the liver surfaces of the control (CON1) group were normal with a dark red in color and no nodules with smooth appearance. The livers of TAA-injected rats were pale in color with scattered nodules on the surface, confirming the induction of fibrosis. After oral administration of *O. octandra*: compared to the fibrosis induced but not treated (INT) livers, the progression of granular nature was reduced with the treatment of CLS and BLE (Figure 3-2 Gross).

To examine the hepatic architecture of the livers, H&E staining was performed. At the end of week 5, the CON1 group showed a regular hepatic architecture with no pathological abnormalities. The fibrosis induced TAA group showed loss of normal architecture with sinusoidal dilation (yellow arrows indicate the development of fibrous bundles around the lobules). At the end of treatment, fibrous bridges were still prominent in the INT group. However, compared to the INT livers, CLS and BLE treated livers showed comparatively less fibrous bridging (Figure 3-2 H&E).

To evaluate the degree of fibrosis in liver samples, collagen fibers in liver tissue were stained with MT. Compared with the CON1, TAA-injections for 5 weeks showed the initiation of deposition of collagen fibers (green arrows). Furthermore, the INT group still showed collagen deposition and incomplete fibrocepata. However, treatment with CLS and BLE for 5 weeks, ameliorated the deposition of collagen fibers compared to the INT group (Figure 3-2 MT).

In addition, TGF-β is a key mediator in the establishment of liver fibrosis. Therefore, immunostaining was performed to determine the localization of TGF-β. Compared to the

CON1, liver sections from the TAA group showed prominent cytoplasmic staining of TGF-β (black arrows). After 5 weeks, the INT group still showed moderate expression of TGF-β. At the end of *O. octandra* treatment, liver sections from CLS and BLE treated rats showed comparatively lower expression of TGF-β compared to the INT group (Figure 3-2 TGF-β IHC).

3-3-2. *O. octandra* leaf extracts improve the biological and biochemical indices of fibrosis progression

The establishment of liver fibrosis and the therapeutic effect of *O. octandra* leaf extracts were observed by monitoring body weight gain (the difference between initial and final body weight) and the liver index (liver/body weight, percentiles). With the induction of liver fibrosis, the TAA group showed a significant decrease in body weight gain compared to the CON1 group at the end of the fibrosis induction period. After treatment, the CLS and BLE treated groups showed a prominent recovery of body weight gain compared to the INT group (Figure 3-3a). At the same time, the TAA group showed a notable increase in liver index compared to the CON1 group at week 5 indicating the establishment of the fibrosis. Notably, the CLS and BLE treatments showed a significant reduction in liver index compared to the INT group (Figure 3-3b).

Induced liver fibrosis and the extent of recovery with *O. octandra* treatment were further evaluated by liver function tests. Serum levels of AST and ALT are markers of liver injury [32]. Therefore, we assessed the degree of liver injury by determining the levels of serum ALT and AST at weeks 5 and 10. AST and ALT were considerably higher in the TAA treated group than in the CON1 group, indicating the establishment of fibrosis at 5 weeks (Figure 3-3c & d). Compared to the start of treatment, the CLS and BLE groups had significantly lower AST levels at the end of week 10, than the INT group (Figure 3-3c). Moreover, the CLS and BLE groups also had notably lower ALT levels than the INT group (Figure 3-3d). These results further confirm that induced fibrosis is restored by treatment with *O. octandra*.

3-3-3. *O. octandra* leaf extracts ameliorate liver fibrosis by mediating key molecular markers of fibrosis

The mRNA expression levels of pro-inflammatory and fibrotic cytokines were examined (Figure 3-4a-c). Compared with the CON1, significantly higher levels of *Tnf-α*, *Tgf-β* and *α-Sma* mRNA expression were observed after induction of the fibrosis with TAA at week 5, confirming the establishment of fibrosis. To evaluate the therapeutic effects of CLS and BLE, the above markers were also analyzed at the end of week 10 (5 weeks of treatment). Interestingly, the expression levels of *Tnf-α*, *Tgf-β* and *α-Sma* were clearly downregulated in the CLS and BLE treated groups compared to INT, but higher than in the CON2 group. These results confirm that both CLS and BLE can be used as a therapeutic option for the liver fibrosis.

3-4. Discussion

Fibrosis is the accumulation of excessive fibrous tissue deposition, that leads to tissue hardening and impaired those function [33]. Chronic inflammation accompanies fibrosis and drives its progression. *O. octandra* plant extracts are being investigated as potential treatments for liver fibrosis and inflammation. Previously we and others have shown that *O. octandra* crude extract has a prophylactic effect curing on liver disease [34,35]. It is also equally important to study the therapeutic effect because it is more important to find the treatment effect after the establishment of liver fibrosis. In this study, as the first step, we conducted an animal study to investigate the therapeutic effect of *O. octandra*. Here before treatment, we established fibrosis in the rat model and after confirming the establishment of fibrosis we treated *O. octandra* and examined the recovery of fibrosis.

Repeated injections of TAA in rats lead to the establishment of fibrosis, resulting in various effects on their physiology [36]. TAA administration reduces appetite, leading to a decrease in caloric intake and subsequent suppression of body weight gain [37]. Concurrently, TAA causes severe liver damage characterized by hepatocyte swelling, glycogen accumulation, and lipid droplet formation [38]. These changes may further induce increased protein synthesis contributing to elevated liver indices [39]. Additionally, AST and ALT activities in the TAA-treated group can be considered as an indicator of liver parenchymal cell damage. Similar findings have been reported in previous studies of TAA-induced liver injury, confirming the establishment of fibrosis [40,41]. As a hepatotoxicant, TAA induces the expression of tumor necrosis factor-alpha (TNF-α), creating a cytotoxic environment that triggers chronic inflammation and progressive liver fibrosis [42]. Another central regulator in chronic liver disease is TGF-β, which contributes to all stages of disease progression by promoting hepatocyte destruction and activating HSCs and fibroblasts [43]. Activation of HSCs can be identified by the

expression of α-SMA, a marker of smooth muscle cell differentiation [44]. Previous studies have also observed elevated inflammatory cytokines and liver damage in TAA-treated rats [45,46].

To study the natural regeneration of the liver after removal of the TAA injection, the INT group was included in the study. Although a slow natural recovery is observed in the INT group, the damage caused by the TAA persists even after removal of the hepatotoxin. This is the critical stage that we need to overcome for the benefit of patients who already have established liver fibrosis. Interestingly, we observed a significant recovery in the treatment of CLS and BLE compared to the natural regeneration. This suggests that the extracts may accelerate the natural regeneration process compared to the natural recovery. This may be due to two reasons: either the leaf extract was involved in the desolation of the fibrous bridges, or the leaf extract prevented the formation of fibrous bridges from the start of the treatment. This is clear evidence establishing the fact that both extracts can effectively heal the liver. These observations of therapeutic recovery were similar to the results of the previously conducted prophylactic studies [35], suggesting that *O. octandra* has both prophylactic effect and therapeutic effect.

These findings suggest that *O. octandra* has hepatoprotective, anti-inflammatory, and anti-fibrotic properties against TAA-induced liver fibrosis. On the other hand, previous studies have shown that the *O. octandra* plant contains a high amount of phenolic compounds, which are rich in antioxidant properties [47–49]. Therefore, it can be hypothesized that the rapid recovery of chronic liver injury may be due to the antioxidants and other supportive compounds present in *O. octandra.* There is a lack of evidence on what kind of phenolic compounds are present in *O. octandra* and how they are intervened in attenuating or reversing of fibrosis.

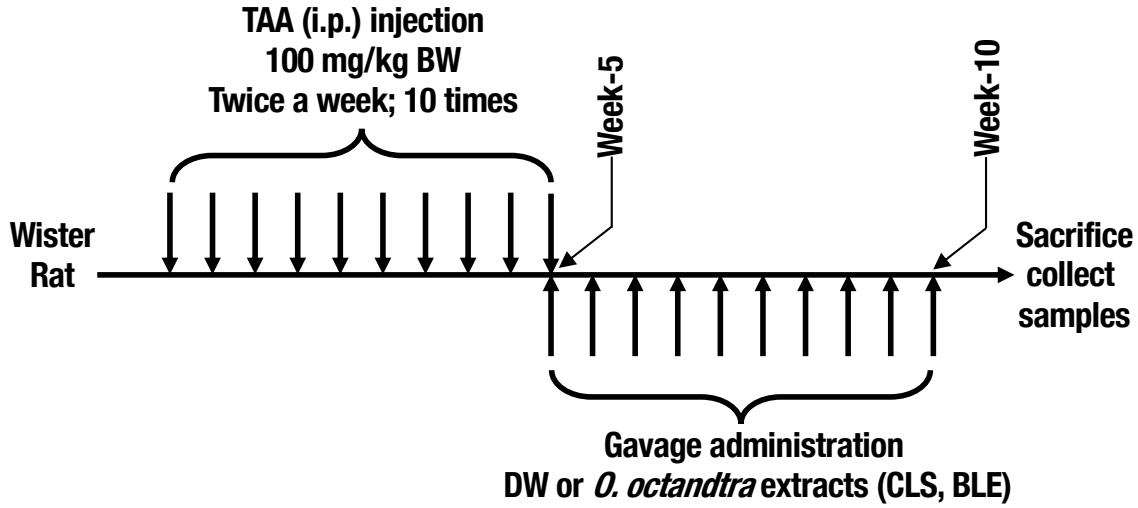

Figure 3-1: Experimental design of an animal study to evaluate the therapeutic effect of CLS and BLE after induction of fibrosis in rats. First fibrosis was induced by injecting TAA at a dose of 100 mg/kg BW, intraperitoneally, twice a week, for 5 weeks. Then rats were treated with CLS or BLE at a dose of 500 mg/kg BW, orally, twice a week. DW (Distilled water) was given to observe the natural regeneration of hepatocytes after chronic liver damage.

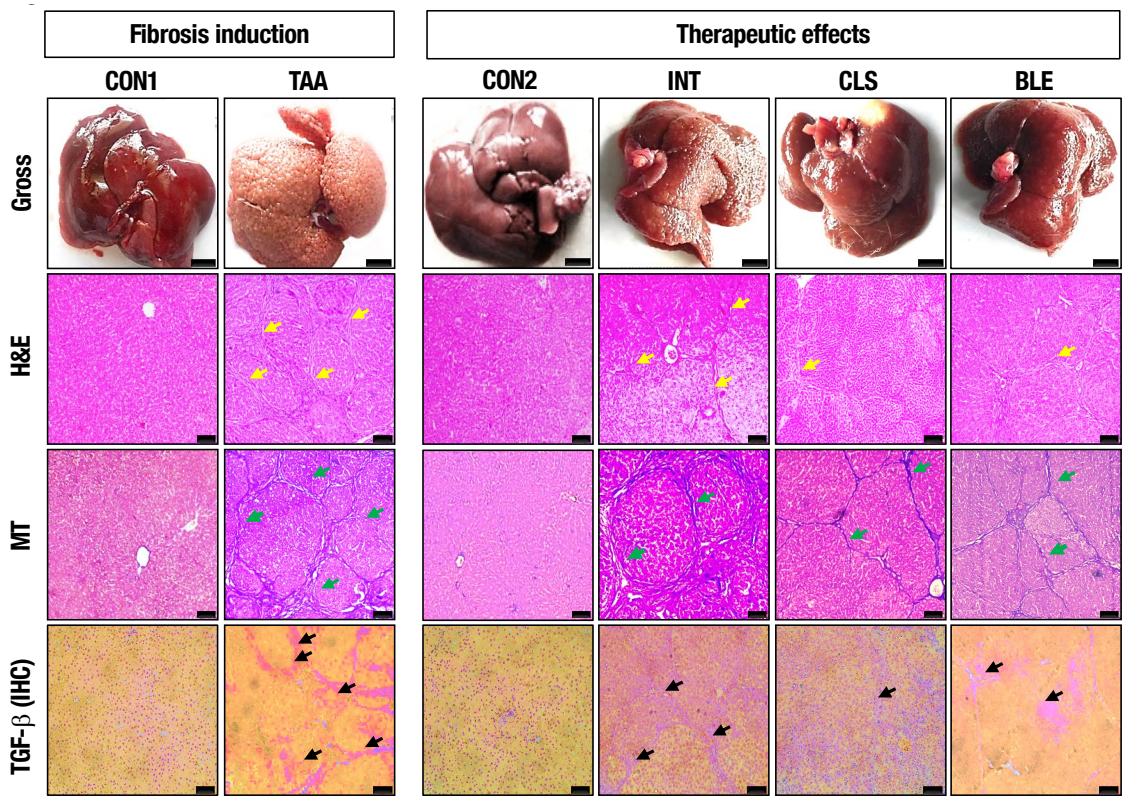

Figure 3-2: Treatment of CLS and BLE improves the restoration of liver. First 2 columns show the induction of fibrosis in TAA group compared to CON1. Next 4 columns show the therapeutic effect of *O. octandra* compared to INT group. First raw shows gross pathological observations. Scale bar=10 mm. Second raw shows improvement in liver architecture (H&E staining). Third raw shows the reduction of the collagen deposition (MT staining). Forth raw shows the ameliorated expression of TGF-β is with the treatment of CLS and BLE. Scale bar=100 µm. Yellow arrows; fibrous bridges, green arrows; collagen deposition and black arrows; TGF-β expression.

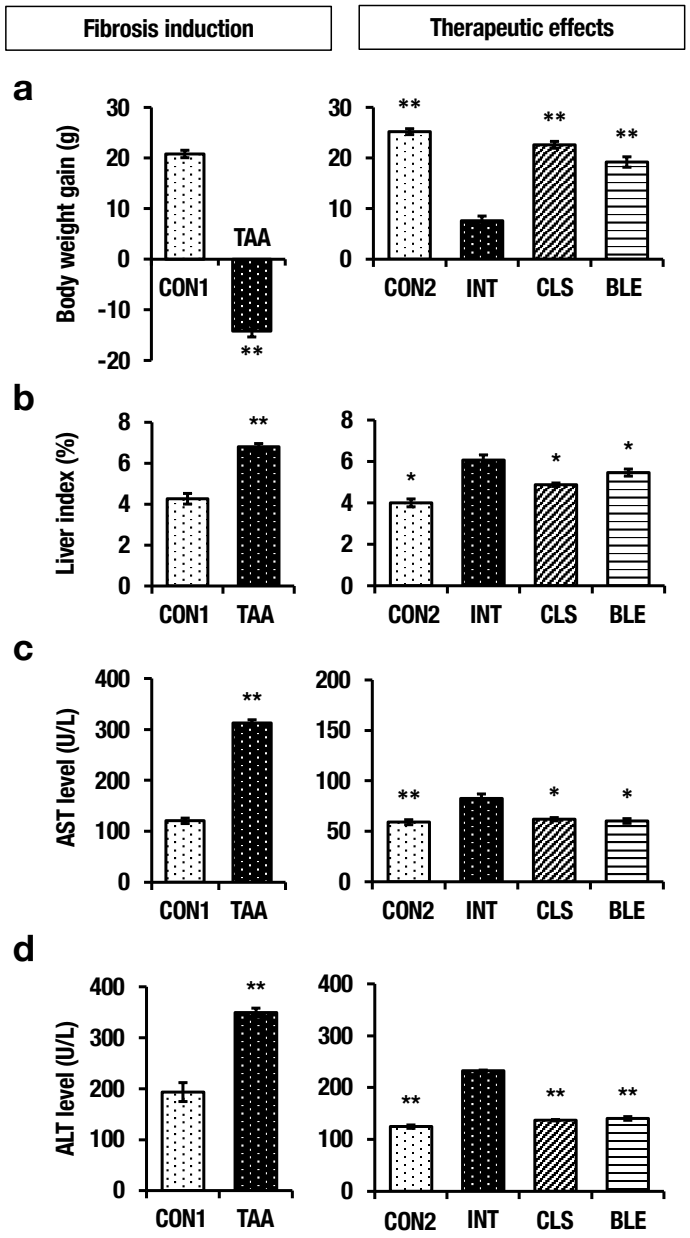

Figure 3-3 : CLS and BLE treatments restore liver condition as measured by body weight, liver weight and serum parameters. (a) Body weight gain after the fibrosis induction and after treatment with CLS and BLE. Values are in grams of increase/decrease from the starting weight. (b) Liver index (Liver/BW ratio), (c) Serum AST levels and (d) Serum ALT levels after the induction of fibrosis and after treatment with CLS and BLE. Statistical significance has been indicated in two ways; (i) disease induction effect during the TAA challenge (CON1 vs. TAA). (ii) treatment's effect (INT vs. CON2, CLS and BLE), with one-way ANOVA followed by Dunnett's test. $*p < 0.05$, $**p < 0.01$. Error bars represent standard errors of the mean (SEM) in each group (n = 5).

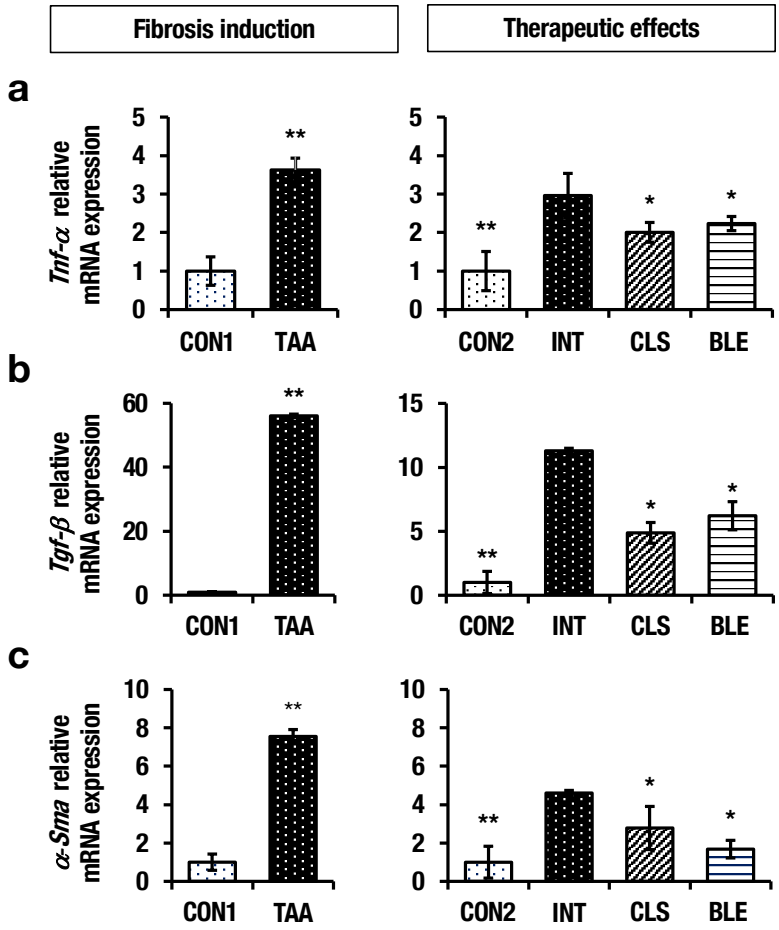

Figure 3-4: CLS and BLE treatments showed hepatoprotective effects by regulating gene expressions in TAA-induced fibrosis. (a-c) Relative mRNA expression of *Tnf-α* (a) *Tgf-β* (b), and *α-Sma* (c) after induction of fibrosis and therapeutic effect after treatment with CLS and BLE. Expression levels are normalized to *18S* rRNA level. Data based on the value from CON1 and CON2 group set as 1.0. The statistical significance has been indicated in two ways; (i) disease induction effect during the TAA challenge (CON1 vs. TAA). (ii) treatment effect (INT vs. CON2, CLS and BLE), with one-way ANOVA followed by Dunnett's test. **p* <0.05, ***p*<0.01. Error bars represent standard errors of the mean (SEM) in each group (n = 5).

CHAPTER 04

Isolation of antifibrotic compound from boiled leaf extract (BLE)

4-1. Introduction

In the preceding chapters, we extensively explored the prophylactic and therapeutic potential of *Osbeckia octandra*. This remarkable plant has been traditionally employed not only for treating liver disorders but also for its immunomodulatory and antimicrobial properties [49,50]. However, comprehensive compound isolation studies are yet to be conducted. Crude extracts typically contain a mixture of compounds, some of which may lack pharmacological activity or could potentially induce undesirable side effects. By isolating and purifying individual compounds from the extract, we can enhance their potency and specificity. This process minimizes the risk of side effects and boosts therapeutic efficacy. The isolation of compounds from crude extracts enables the production of pure and standardized substances with consistent potency and purity. This ensures accurate dosing and reduces variability between batches. By isolating and purifying individual compounds, we can achieve improved pharmacokinetic profiles, including enhanced bioavailability, prolonged half-life, and reduced toxicity. Such findings contribute to a deeper understanding of the natural world and may lead to the discovery of novel compounds with therapeutic potential.

Therefore, in this chapter, our primary focus is on the isolation and identification of compounds associated with the antifibrotic effect observed in the *O.octandra* crude extract. Additionally, we aim to investigate the potential of its antifibrotic effect and elucidate the underlying regulatory pathways.

4-2. Experimental section

4-2-1. Fractionation of BLE

BLE was prepared by mixing 300 g of freeze-dried powder with 2.4 L of DW and boiling for 20 min. The supernatant was re- moved, and the solvent was concentrated *in vacuo* and passed through a column of DIAION HP20SS (Mitsubishi Chemical, Tokyo, Japan), which was eluted with DW containing increasing amounts of methanol.

4-2-2. Thin layer chromatography

Thin layer chromatography (TLC) was performed on precoated 0.2 mm thick Kieselgel 60 F254 plates (Merck) were developed with chloroform/methanol/water (8:5:1, v/v/v), or toluene/ethyl formate/fomic acid (1:7:1, v/v/v). Spots were detected under UV illumination after spraying with 2% ethanolic FeCl3 or 5% sulfu- ric acid and heating.

4-2-3. HPLC analysis

High performance liquid chromatography (HPLC) was used to identify the peaks for BLE, each fraction (F1–F4) and isolated compounds by using an LC-20AT HPLC system (Shimadzu, Ky- oto, Japan) equipped with a COSMOSIL Cholester, 4.6 mm I.D. × 250 mm, reversed-phase column (Nacalai Tesque, Kyoto, Japan). The mobile phase was 0.1% formic acid/H2O—CH3CN (10%– 80% in 30 min with linear gradient elution) at a flow rate of 0.6 mL/min, temperature 40 °C, and the absorbance of the ef- fluent solution was measured from 200 to 700 nm using an SPD- M20A photodiode array detector (Shimadzu).

4-2-4. Cell culture

The human hepatic stellate cell line LX-2 was donated by Dr. Scott L. Friedman (Mount Sinai School of Medicine, New York, NY, USA) and was cultured in high glucose Dulbecco's modified eagles medium (DMEM) (Fujifilm Wako, Osaka, Japan) supplemented with 10%

fetal bovine serum (FBS) (Equitec-Bio, Kerrville, TX, USA), 100 U/mL penicillin and 100 μg/mL streptomycin (Nacalai Tesque) in a humidified atmosphere containing 5% CO_2 at 37°C.

4-2-5. Cytotoxicity and cell viability assay

LX-2 cells (4.0×10^4 cells/well) were seeded in a 96-well plate and incubated for 16 h. The medium was replaced with fresh medium containing *O. octandra* fractions or isolated compounds. The cells were then stimulated for 24 h and to analyze cell viability, the medium was replaced with fresh medium containing 1/10 (v/v) of CCK-8 assay reagents (Dojindo, Kumamoto, Japan) and incubated for 1 h. After incubation, the OD_{450} of the CCK-8 reagents was measured using the SpectraMax i3x (Molecular Devices, San Jose, CA). Cell viability was expressed as a percentage of cells stimulated with 1% dimethyl sulfoxide (DMSO) and used as a negative control.

4-2-6. Induction strategy for to identify antifibrotic effect

LX-2 cells were activated with 10% FBS for 24 hours to induce fibrosis and then different fractions were treated for 24 hours. To compare the treatment effect three controls were maintained: to observe the activation of LX-2, fibrosis induced group (control F); treated with 10% FBS only, to observe the restoration from active to inactivate (quiescent) state, gradually recovered group (control R); treated with 2% FBS and to observe the clinically available drug, treatment positive group (control T); treated with 5 μM of doxorubicin (Toronto Research Chemicals, Toronto, ON, Canada) for 24 hours (Figure 4b). The antifibrosis effect of each fraction was determined by examining the fibrotic markers; TGF-β, α-SMA, COL1A1, CD44, SMAD2/3 and SMAD7.

4-2-7. Isolation and identification of major bioactive compounds

Based on the results of the antifibrotic study for F1 - F4, we selected F3 and F4 for further purification. To purify these fractions, we used a stepwise elution process with DW and methanol using Sephadex LH20 (Sigma, St. Louis, MO, USA) and TOYOPEARL HW-40F (Tosoh, Tokyo, Japan) as the purification medium. To identify the peaks of the purified compounds, nuclear magnetic resonance (NMR) spectra were obtained using an ADVANCE NEO 400 spectrometer (Bruker, Billerica, MA, USA) to identify the isolated compounds. DMSO-*d*6 was used as a solvent for CSU and GA, methanol-*d*4 for PDN. For further confirmation of PDN and CSU, high resolution electrospray Ionization-Mass Spectrometry (HRESI-MS) analysis was done for the confirmation of PDN and CSU with high resolution mass spectrometer, micrOTOF II (Bruker). The mass spectrometer conditions were capillary voltage 3.5 kV, desolvation temperature 200°C, gas flow 4 L/min, and gas pressure 0.3 bar. Nitrogen was used as drying and collision gas, respectively. The data were analyzed using the Data Analysis 4.1 software (Bruker).

4-2-8. Immunoblot analysis

The LX-2 cells (5.0 × 105 cells/well) were seeded in a 12- well plate and cultured in 10% FBS for 24 h. The medium was then replaced with a fresh medium containing differ- ent concentrations of *O. octandra* fractions or isolated com- pounds and stimulated for 24 h. After stimulation, the cells were lysed with sodium dodecyl sulphate (SDS) sample buffer (125 mM Tris-HCl, pH 6.8, 100 mM DTT, 2% [w/v] SDS, 5% [w/v] sucrose, 0.002% [w/v] bromophenol blue), centrifuged at 13000 rpm for 5 min, and boiled at 90 °C for 5 min. The sam- ples were subjected to SDS-polyacrylamide gel electrophoresis and transferred to polyvinylidene fluoride membranes (Fujifilm Wako). The membranes were blocked and incubated with pri- mary antibodies against α-SMA, TGF-β, COL1A1, CD44, and SMAD2/3 (Cell Signaling

Technology, Danvers, MA, USA), or β-actin (Fujifilm Wako). The membranes were then washed and incubated with horseradish peroxidase (HRP)-conjugated secondary antibodies. Signals were detected with ImmunoS- tar LD (Fujifilm Wako) using Lumino Graph I (ATTO, Tokyo, Japan).

4-2-9. RNA isolation and quantitative PCR

Total RNA from the mouse liver and the cells was extracted using Sepasol RNA I Super G (Nacalai Tesque) according to the manufacturer's instructions. The extracted RNA was then reverse transcribed using the FastGene cDNA Synthesis x ReadyMix (Nippon Genetics, Tokyo, Japan). The resulting cDNA was used as a template for quantitative PCR (qPCR) using the KAPA SYBR Fast qPCR Master Mix (Kapa Bioscience, Potters Bar, UK) with the Mx3005P qPCR system (Agilent Technologies, Santa Clara, CA, USA). The primers used for this study are listed in Table 1. The 18S rRNA expression was used as an internal control to normalize the mRNA expression data [51,52].

4-2-10. Immunohistochemistry

Immunohistochemistry for TGF-*β* in liver sections was performed according to the protocol described herein. Briefly, dewaxed and rehydrated tissue sections were blocked and then incubated with TGF-*β* antibody (Abcam, Cambridge, UK) antibody at 4°C for 24 hours. They were incubated with Dual Link System-HRP labeled secondary antibody (Agilent Technologies) for 30 min at room temperature and visualizing according to the manufacture's recommendations. The slides were then mounted with a coverslip. Photographs were taken using an IX73 inverted microscope, and digital images were captured using DP27, and analyzed with CellSense software (Olympus, Tokyo, Japan).

Immunofluorescence for CD44 was performed according to a previously published protocol [53]. Briefly, LX-2 cells were cultured and treated in chamber slides and the cells were prefixed with

formaldehyde and permeabilized with Triton X-100. The cells were then incubated with anti-CD44 antibodies (Cell Signal Technology) overnight at 4°C. The cells were then washed three times with 1× PBS. DyLight488 conjugated goat anti-mouse-IgG (Bio-Rad, Hercules, CA, USA) was added as a secondary antibody and incubated for 1 hour at room temperature. This was followed by co-staining with PureBlu DAPI nuclear staining dye (Bio-Rad). Finally, images were captured using an DMi8 inverted microscope and processed using the THUNDER imaging system (Leica Microsystems, Wetzlar, Germany).

4-2-11. Statistical analyses

Statistical analyses were performed using one-way analysis of variance (ANOVA) with a Dunnett's test. Data are expressed as mean ± standard error of the mean (SEM) or mean ± standard deviation (SD).

4-3. Results

4-3-1. Bulk fractionation for the identification of anti-fibrotic compounds in *O. octandra* boiled leaf extract

To identify possible bioactive compounds which are responsible for the therapeutic effect, BLE was fractionated by column chromatography (DIAION as stationary phase and aqueous methanol as mobile phase). At the end of this process, the eluates were separated into four fractions (dry weights for F1 - F4 were 26, 8.0, 3.0 and 8.0 g, respectively) based on the spots on the TLC plate after spraying anisaldhyde and/or $FeCl_3$ under UV light.

4-3-2. LX-2 fibrosis model allows identification of the antifibrotic fraction from boiled leaf extract

To evaluate the antifibrotic effect of each fraction, the LX-2 cell line was used. The LX-2 cells show characteristics of primary HSCs in vivo and shows a quiescent (inactivated) phenotype in growth medium with low serum concentrations (2% FBS) but gets activated in high serum concentrations (10% FBS). To activate quiescent LX-2 cells, they were cultured in 10% FBS for 24 hours. This activation mimics the fibrosis in HSCs. Different fractions were then used to treat the cells at different doses for another 24 hours (Figure 4-1).

To select the best concentration series to study the therapeutic effect of each fraction, cell viability and IC_{50} values were examined using the CCK-8 assay. As shown in the Figure S1a cell viability decreased in a dose-dependent manner. Calculated IC_{50} values for F1; 1,362, F2; 2,016 F3; 890, and F4; 1,621 μg/mL, respectively (Figure 4-2a & b). According to these values, three doses; 1,000, 500 and 250 μg/mL were selected to evaluate the antifibrosis effect of each of the fractions. Protein expression of key fibrotic markers was also examined. According to the immunoblotting results (Figure 4-3c), with respect to the three controls used in this study, the continuous fibrosis induced group (control F) showed significantly higher TGF-β, α-SMA and colagen1 α1 (COL1A1) protein expression levels compared to the gradually recovered

group with 2 % FBS treatment (control R), confirming the activation of HSCs. Notably, after the treatments, F3 and F4 showed remarkably lower expression levels of fibrotic markers: TGF-β, α-SMA and COL1A1, compared to F1 and F2 (Figure 4-3d-f). Furthermore, the strongest antifibrotic effect could be observed in F3 and F4 compared to control R and the positive control (control T) treated with doxorubicin. Based on these results, F3 and F4 were used for further isolation of bioactive compounds responsible for the antifibrotic effect.

4-3-3. Pedunculagin, casuarinin and gallic acid were identified as compounds from fractions 3 and 4

BLE and fractions (F1 - F4) were analyzed by HPLC and the profiles are shown in Figure 4-4 a-e. To identify the major compounds, present in F3 and F4, the fractions were chromatographed, and three compounds were isolated. These isolated compounds were confirmed as pedunculagin (PDN), casuarinin (CSU), and gallic acid (GA) by HRESI-MS (PDN and CSU) and NMR (PDN, CSU and GA) analyses. The profiles for the isolated compounds (retention times: PDN (13.7 and 16.7 min, for a and b-isomer) [54], CSU (18.6 min) [55] and GA (7.9 min) [56] are also shown in Figure 4-4 f-h.

Pedunculagin (PDN):

HRESI-MS (positive-ion mode) m/z: 807.0648 [M+Na] + (calcd for $C_{34}H_{24}NaO_{22}$, 807.0657). ^{1}H NMR (400 MHz, CD_3OD):δ H 3.82 (1H, brd, *J* = 11.5 Hz, H-6b α anomer), 3.88 (1H, brd, *J* = 12.6 Hz, H-6b β anomer), 4.15 (1H, m, H-5 β anomer), 4.58 (1H, m, H-5 α anomer), 4.95 (1H, d, J = 8.1 Hz, H- 1 β anomer), 5.07-5.12 (4H, unresolved, H-2 α, β anomers and H-4 α, β anomers), 5.25-5.33 (3H, unresolved, H-3 β anomer and H-6a β, α anomers), 5.36 (1H, d, *J* = 4.0 Hz, H-1 α anomer), 5.47 (1H, t, *J* = 9.6 Hz, H-3 glucose α anomer), 6.35, 6.36, 6.49, 6.52, 6.58, 6.60, 6.61 (s, HHDP-H). ^{13}C NMR (125 MHz, CD_3OD): δC 62.7 (Glu C-6ab), 66.4(Glu C-5a), 68.5 (Glu C-4a), 69.0 (Glu C-5b), 71.9 (Glu C-4b), 75.0 (Glu C-2a), 75.8 (Glu C-3b),

76.7 (Glu C-3a),77.3 (Glu C-2b), 90.8 (Glu C-1a), 94.4 (Glu C-1b), 106.3, 106.4, 106.7, 107.2 (HHDP C-3), 113.5, 115.2 (HHDP C-1), 124.6, 124.9, 125.0 (HHDP C-2), 136.1 (HHDP C-5), 143.5, 144.4 (HHDP C-4,6), 167.7, 168.1, 168.3, 168.8, 169.4 (HHDP COO) (Figure 5-5a).

Casuarinin (CSU):

HRESI-MS (positive-ion mode) m/z: 959.0877 [M+Na]+ (calcd for C41H28NaO26, 959.0767). ^{1}H NMR (400 MHz, DMSO-d_6): δ H 3.96 (1H, d, J = 12.8 Hz, Glu H-6a), 4.53 (2H, m, Glu H-2, H-6b), 5.15-5.23 (3H, m, Glu H-3, H-4, H-5), 5.37 (1H, br.s, Glu H-1), 6.23, 6.28, 6.56 (each 1H, s, HHDP protons), 6.92 (2H, s, galloyl protons). ^{13}C NMR (125 MHz, DMSO-d_6): δC 64.3 (Glu C-6), 66.1 (Glu C-1), 68.8 (Glu C-3), 70.0 (Glu C-5), 73.4 (Glu C-4), 75.8 (Glu C-2), 103.6, 105.0, 106.6 (HHDP C-3), 109.2 (galloyl C-2,6), 114.8, 115.8, 116.3, 116.7 (HHDP C-1 and HHDP C-3, for HHDP attached to C-1 glu), 119.1 (galloyl C-1), 119.6, 123.1, 125.4, 126.1 (HHDP C-2), 134.3, 135.0, 136.5, 138.1 (HHDP C-5), 139.4 (galloyl C-4), 143.0, 144.7, 144.8 (x2), 145.2, 145.3, 145.4, 146.0 (HHDP C-4,6), 145.4 (galloyl C-3,5), 163.8 (galloyl COO), 164.9, 168.2, 168.7, 169.4 (HHDP COO) (Figure 5-5b).

Gallic acid (GA): ^{1}H NMR (400 MHz, DMSO-d_6): δH 6.92 (2H, s, galloyl protons) (Figure 5-5c).

4-3-4. Restoration of fibrosis is confirmed with key fibrotic markers in activated HSCs by pedunculagin, casuarinin and gallic acid.

To evaluate the antifibrotic activity of the isolated and identified compounds, previously established cell culture model was used (Figure 4-1). Cells were treated at three different doses of 25, 50 and 100 μM. Subsequently, key fibro genetic markers were studied as in previously (TGF-β, α-SMA and COL1A1). In addition, we performed immunoblot analysis of cluster of differentiation 44 (CD44) expression which is reported as a newly identified fibrotic marker (Figure 4-6a). Prior to examining PDN, CSU and GA activity, the expression profiles of 4

fibrotic makers were compared between the controls F, R and T in the LX-2 cell model. Control R and T groups showed noticeably lower TGF-β, α-SMA, and COL1A1 expression compared to control F (Figure 4-6b-d). In the CD44 expression profile, control R showed similar CD44 expression to control F, whereas the treatment positive group control T showed a significant downregulation of CD44 expression (Figure 4-6e). The TGF-β, α-SMA, COL1A1 expression was downregulated by PDN, CSU, and GA treatment in a dose-dependent manner compared to the control F (Figure 4-6b-d). CD44 expression level was clearly downregulated by PDN, CSU and GA treatment, with prominent downregulation was observed at the high dose (Figure 4-6e). These results suggest that PDN, CSU, and GA have great potential for the treatment of liver fibrosis.

To understand the effect of these isolated compounds on the gene expressions of the above fibrogenesis markers, mRNA expressions were also studied (Figure 4-7a-d). Consistent with the immunoblot results, PDN, CSU and GA treatment at high and medium doses showed significant downregulation of *TGF-β, α-SMA*, and *CD44* compared to the control F (Figure 4-7a, b, d). In addition, *COL1A1* expression was downregulated in a dose-dependent manner in all three treatments (Figure 4-7c). Notably both the control R and T showed significant downregulation of *TGF-β, α-SMA* and *COL1A1*compared to the control F. Taken together, PDN, CSU and GA showed a significant therapeutic effect in activated LX-2 cells.

To further confirm the fibrotic treatment marker CD44, immunofluorescence studies were performed. A medium dose (50 μM) was selected to study the effect of each isolated compound on CD44 expression (Figure 4-8). Control F showed significantly higher expression of CD44 in the cytoplasm compared to both control R and T. Treatment with PDN, CSU and GA resulted in remarkably lower cytoplasmic expression of CD44 compared to the control F, visually demonstrating the therapeutic effect and confirming the immunoblot results.

4-3-5 Pedunculagin, casuarinin and gallic acid show anti-fibrotic effects through TGF-*β*/SMAD signaling pathway

In the antifibrotic study, we and others have reported the significant downregulation of TGF-β at both protein and mRNA expression levels [57]. Therefore, we further investigated the downstream signaling pathway of TGF-*β*/SMAD signaling, which is a key pathway leading to liver fibrosis (Figure 4-9a). As shown in Figure 4-9b and c, significant downregulation of both SMAD2 and SMAD3 was observed with PDN treatment in a dose-dependent manner. CSU and GA showed significant downregulation at high and medium doses compared to the control F. In addition, control T also showed significantly low expression of SMAD2 and SMAD3 proteins compared to the control F.

The mRNA expressions also clearly showed that PDN, CSU and GA downregulated *SMAD2* (Figure 4-10a) and *SMAD3* (Figure 4-10b), to mediate fibrosis, which is negatively regulated by *SMAD7*, an inhibitory protein for TGF-*β* signaling. We then examined the mRNA expression of *SMAD7*. As shown in Figure 4-10c, *SMAD7* is clearly increased in response to treatment of PDN, CSU and GA compared to the control F. Taken together, PDN, CSU and GA showed a potential therapeutic effect via intervention of TGF-*β*/SMAD signaling in liver fibrosis.

4-4. Discussion

In this study, we established an *in vitro* model to screen for antifibrotic compounds. We focused on HSCs because they are crucial and initial players in liver fibrosis. Normally these cells are in a quiescent state, and they get activated in response to liver injury [58]. This activation is stimulated by factors such as TGF-β, which binds to specific receptors and triggers signaling pathways that lead to phenotypic changes and the transformation of HSCs into myofibroblast-like cells [59]. This activation increases the expression of α-SMA and stimulates the production and accumulation of collagen, ultimately contributing to the development of liver fibrosis [60]. Therefore, finding ways to intervene in the activation of HSCs is crucial to prevent or reverse liver fibrosis and protect the liver from further damage. Here, we used an immortalized human HSC cell line, LX-2, which allows for accessible in-depth mechanistic investigations without the use of cancer cell lines or animal models [61,62]. Typically, these LX-2 are treated with (carbon tetrachloride) CCl_4 or TGF-β to induce fibrosis *in vitro*. LX-2 cells show an inactivated (quiescent) state under 2% low serum conditions. In the presence of 10% high serum, LX-2 cells are activated and formed fibrotic feature, making it an accessible model to study HSCs activation without the need for CCl_4 or TGF-β [63,64].

Secondly, as for the first time, we were able to isolate the antifibrotic compounds, pedunculagin (PDN), casuarinin (CSU) and gallic acid (GA) from the BLE of *O. octandra* using the LX-2 antifibrotic agent screening system. PDN and CSU are polyphenols belonging to the group of hydrolysable ellagitannins which generate ellagic acid by oxidative degradation [65,66]. Furthermore, this is the first time that PDN and CSU have been isolated from *O. octandra*. However, the effect of ellagitannin on liver fibrosis remains largely unknown. All though, GA has already been identified as a hepatoprotective agent [67], we compared the effect of PDN and CSU effect with GA. Interestingly, treatment with PDN and CSU reduced the transcription of α-SMA and COL1A1, showing significant intervention via the TGF-β signaling pathway. This

observation may be due to the prevention of transcription of fibro genic genes and preventing the synthesis and deposition of ECM components in the liver [68]. As a result, activated HSCs may prevent further activation or revert to their inactivated form suggesting the therapeutic potential. In addition, here to compare the antifibrosis effect with natural recovery and doxorubicin witch one of the potential drug available in the market for liver fibrosis as mentioned above. Prominent antifibrosis effect could be observed for *O. octandra* suggesting significant therapeutic potential.

In this study, we investigated the expression of CD44, a newly identified fibrosis marker, during the treatment with our isolated compounds. CD44 is expressed on the surface of HSCs and has been found to be upregulated during HSCs activation in liver fibrosis [69]. In addition, CD44 has been associated with HSCs survival and resistance to apoptosis [70], which may contribute to the persistence of activated HSCs and the progression of liver fibrosis. Notably, PDN and CSU showed remarkable intervention on CD44 expression in activated LX-2 cells suggesting treatment potential to remove activated HSCs by transforming them into an inactivated form. Furthermore, PDN and CSU could accelerate the natural transformation of activated HSCs into their inactivated form by preventing the progression of fibrosis. These findings suggest that PDN and CSU may interfere with the activation of HSCs via the TGF-β signaling pathway.

As mentioned above, during the induction of fibrosis in HSCs, TGF-β induces conformational changes in SMAD2/3 in the cytoplasm, leading to its release from the receptor complex and binding to SMAD4 to form the SMAD2/3 complex, which then catalyze the phosphorylation of the serine residue on the downstream SMAD molecule [71]. The phosphorylated SMAD then enters the nucleus and regulates the expression of TGF-β targets such as α-SMA and COL1A1, further inducing the onset of fibrosis [72]. The SMAD family includes at least nine proteins,

expressed as SMAD1-9, which are subdivided into receptor-activated SMAD (R-Smad), common pathway SMAD (Co-Smad), and inhibitory SMAD (I-Smad). R-Smad, such as SMAD2 and SMAD3, are mainly known to promote liver fibrosis, whereas I-Smad, such as SMAD7 can inhibit or regulate the TGF-β family of signal transduction and inhibit liver fibrosis [73]. Since the TGF-β/SMAD signaling pathway plays such an important role in liver fibrosis, blocking or mediating its signaling is an important potential strategy to prevent and treat liver fibrosis [74]. Interestingly, PDN, CSU and GA downregulated *SMAD2* and *SMAD3* and upregulated *SMAD7*, thereby inhibiting the TGF-β/SMAD signaling pathway. In addition, our data indicate that natural gradual recovery of HSCs may require more time for recovery, suggesting that PDN and CSU have more potential to recover fibrosis than natural recovery and doxorubicin.

In conclusion, the present study demonstrates the possible therapeutic potential of *O. ocatndra* to cure fibrosis via mediation of the TGF-β/SMAD signaling pathway and sheds light on the clinical significance for the other inflammatory diseases as well.

Table 4-1: Primers used for qPCR in this *chapter*

Gene	Sequence
Human-TGF-β	F; 5′–TACCTGAACCCGTGTTGCTCTC–3′ R; 5′–GTTGCTGAGGTATCGCCAGGAA–3′
Human-α-SMA	F; 5′–GCTGAAGTATCCGATAGAACACG–3′ R; 5′–GGTCTCAAACATAATCTGGGTCA–3′
Human-CD44	F; 5′–GCTTCCAGAGTTACGCCTTGA–3′ R; 5′–AACCCTTGCAACATTGCCTGA–3′
Human-COL1A1	F; 5′–GTACTGGATTGACCCCAACC–3′ R; 5′–CGCCATACTCGAACTGGAAT–3′
Human-SMAD2	F; 5′–CCGACACACCGAGATCCTAAC–3′ R; 5′–AGGAGGTGGCGTTTCTGGAAT–3′
Human-SMAD3	F; 5′–CCATCTCCTACTACGAGCTGAA–3′ R; 5′–CACTGCTGCATTCCTGTTGAC–3′
Human-SMAD7	F; 5′–CTCGGACAGCTCAATTCGGA–3′ R; 5′–CAGTGTGGCGGACTTGATGA–3′
Human-18S	F; 5′–GTAACCCGTTGAACCCCATT–3′ R; 5′–CCATCCAATCGGTAGTAGCG–3′

[a] F; forward primer. [b] R; Reverse primer.

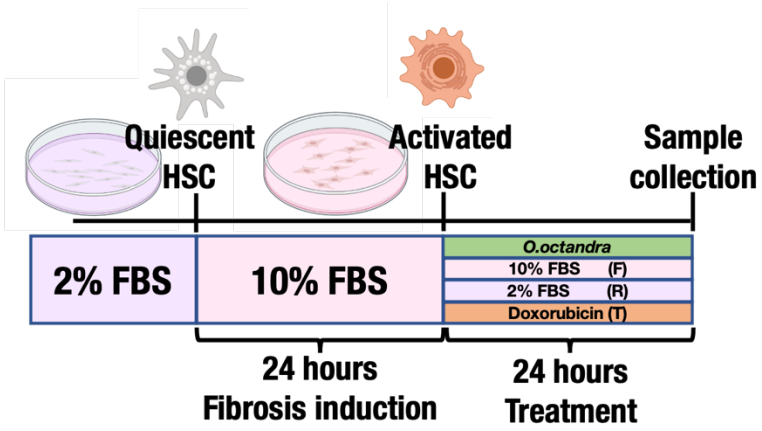

Figure 4-1. Cell culture model established in LX-2 cells to screen the antifibrotic effect. LX-2 cells show its quiescent (inactivation) form under the low serum condition (2% FBS). Quiescent LX-2 cells were activated in high serum condition (10% FBS) to induce the fibrosis. Activated LX-2 cells were treated with different concentrations of *O. octandra* and 3 controls, fibrosis induced group (F); treated with 10% FBS only, gradually recovered group (R); treated with 2% FBS and treatment positive group (T); treated with 5 μM of doxorubicin) for 24 hours.

a

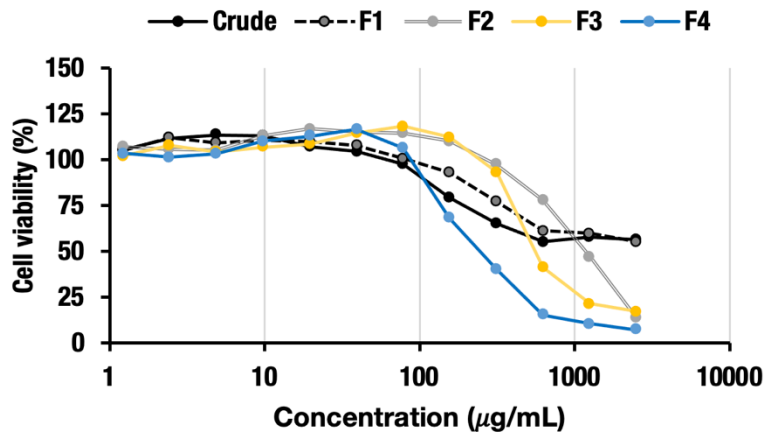

b

Calculated IC_{50} values for each fractions

Fraction	IC_{50} Value (μg/mL)
Crude	1,408
F1	1,362
F2	2,016
F3	890
F4	1,621

Figure 4-2: Cytotoxic effect of crude extract and different fractions of BLE on activated HSC line LX-2. (a) CCK-8 assay to evaluate the cell viability of BLE (crude) and its fractions (F1-4). The percentage of cell viability is represented by the value of 1% DMSO treated cells as 100% viability. (b) Calculated IC_{50} values for BLE and F1-4. These values were calculated using the trend line equation (y=mx+n, in this equation y=50 value x point becomes IC_{50}).

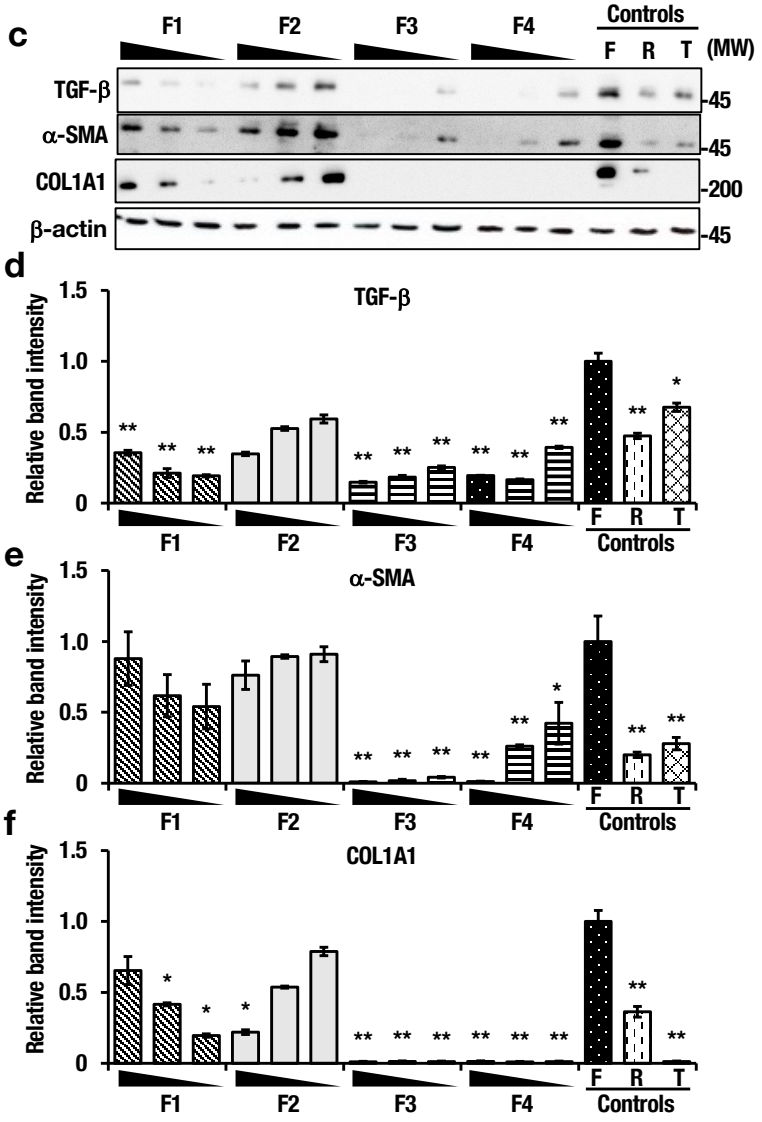

Figure 4-3: Fraction 3 and 4 showed antifibrotic effect by reducing the expression of fibrotic markers in activated HSCs. Immunoblot analyses of key fibro genetic markers: activated LX-2 cells were treated with various concentrations (1,000, 500 and 250 μg/mL) of different fractions (F1-4) and fibrosis induced group (F); treated with 10% FBS only, gradually recovered group (R); treated with 2% FBS and treatment positive group (T); treated with 5 μM of doxorubicin) for 24 hours. Equal loading was sassed by probing the blots with antibody against β-actin. (d-f) Relative band intensity of TGF-β (d), α-SMA (e), and COL1A1 (f). Band intensities were measured with image J software. Data based on the value from control F set as 1.0. *p <0.05, **p <0.01 (one way ANOVA with Dunnett's test). Each data is mean ± SD (n=3).

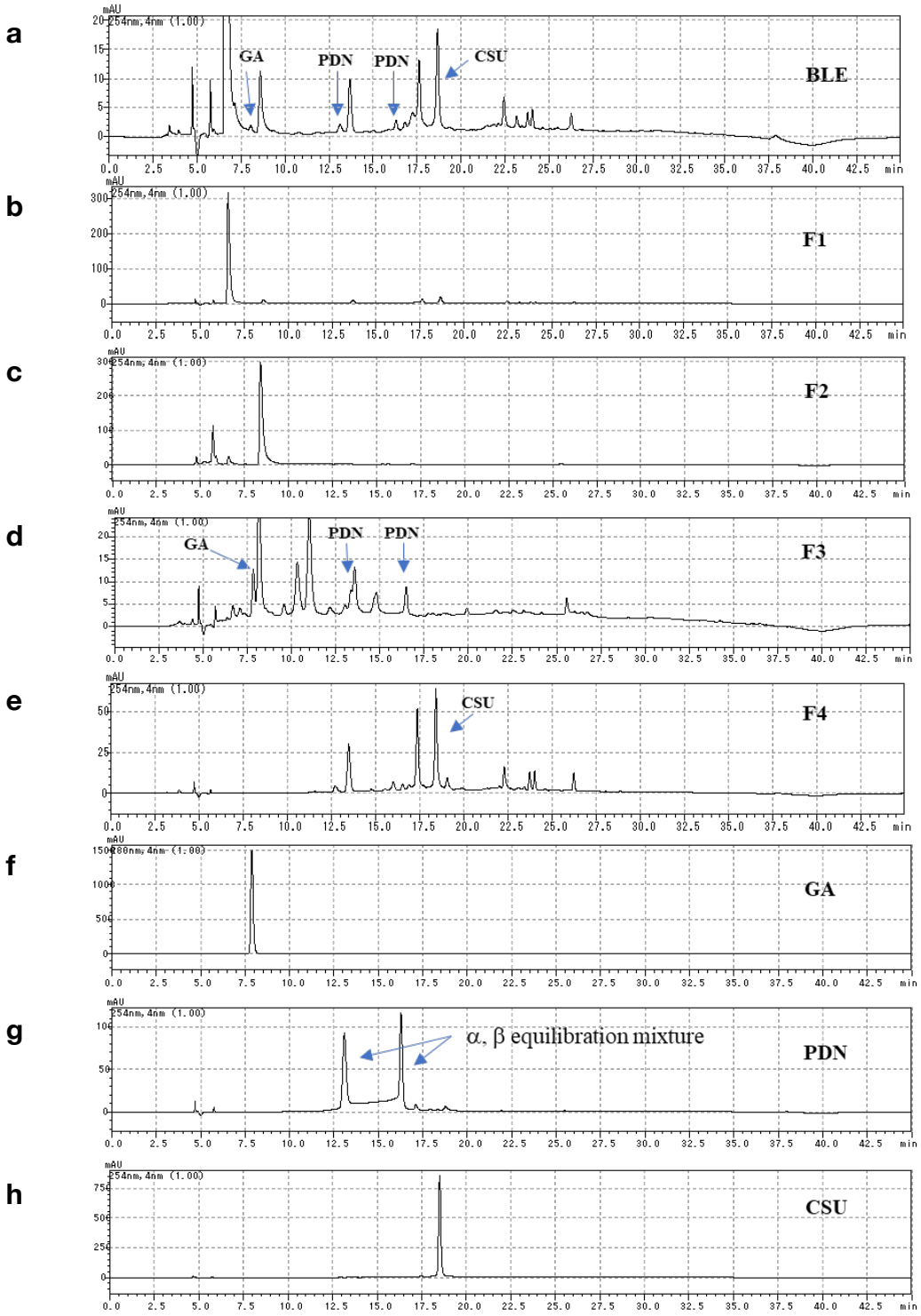

Figure 4-4: Pedunculagin, casuarinin and gallic acid identified as major bioactive compounds in BLE of *O. octandra*. (a) HPLC profiles of the BLE. (b-e) HPLC profiles of each fraction (F1-F4). (f-h) HPLC profiles of isolated compound; pedunculagin (PDN), casuarinin (CSU) and gallic acid (GA).

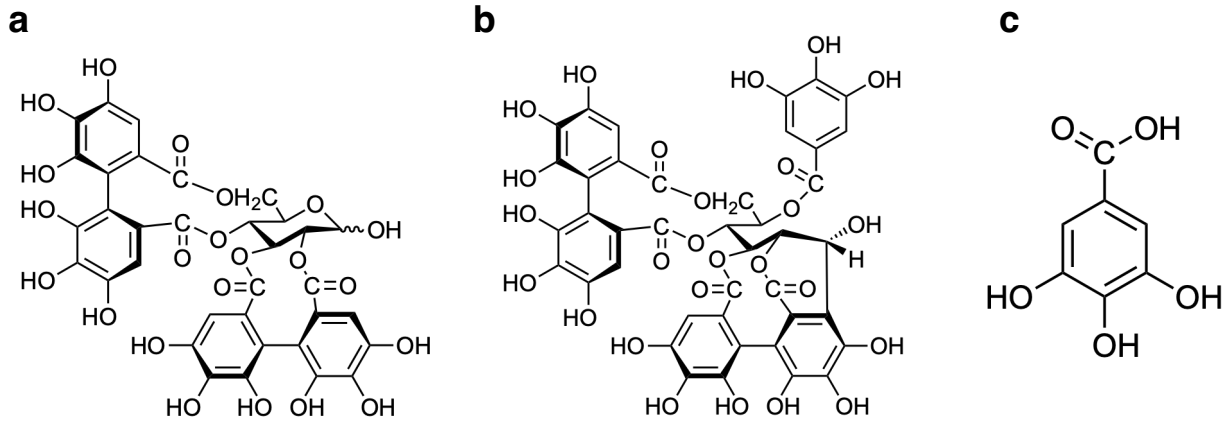

Figure 4-5: Chemical structure of Pedunculagin, casuarinin and gallic acid

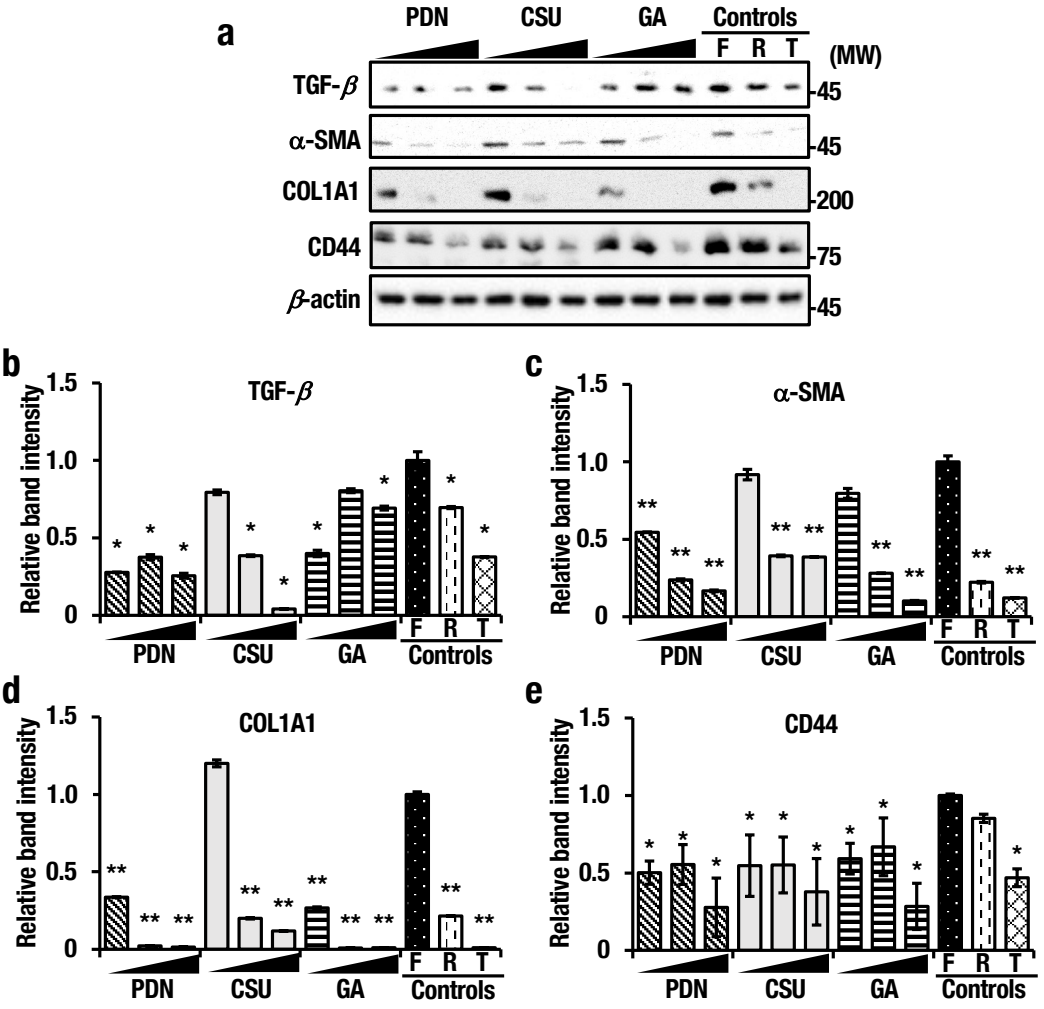

Figure 4-6: Pedunculagin, casuarinin and gallic acid mediate fibrosis via regulation of key fibrotic markers. (a) Immunoblot analyses of key fibro genetic markers: activated LX-2 cells were treated with different concentrations (25, 50 and 100 μM) of different isolated compounds and controls (fibrosis induced group (control F); treated with 10% FBS only, gradually recovered group (control R); treated with 2% FBS and treatment positive group (control T); treated with 5 μM of doxorubicin) for 24 hours. Equal loading was sassed by probing the blots with antibody against *β*-actin. (b-c) Relative band intensity of TGF-*β* (b), α-SMA (c), COL1A1 (d), and CD44 (e). Band intensities were measured with image J software. Data based on the value from control F set as 1.0. **p* <0.05, ***p* <0.01 (one way ANOVA with Dunnett's test). Each data is mean ± SD (n=3).

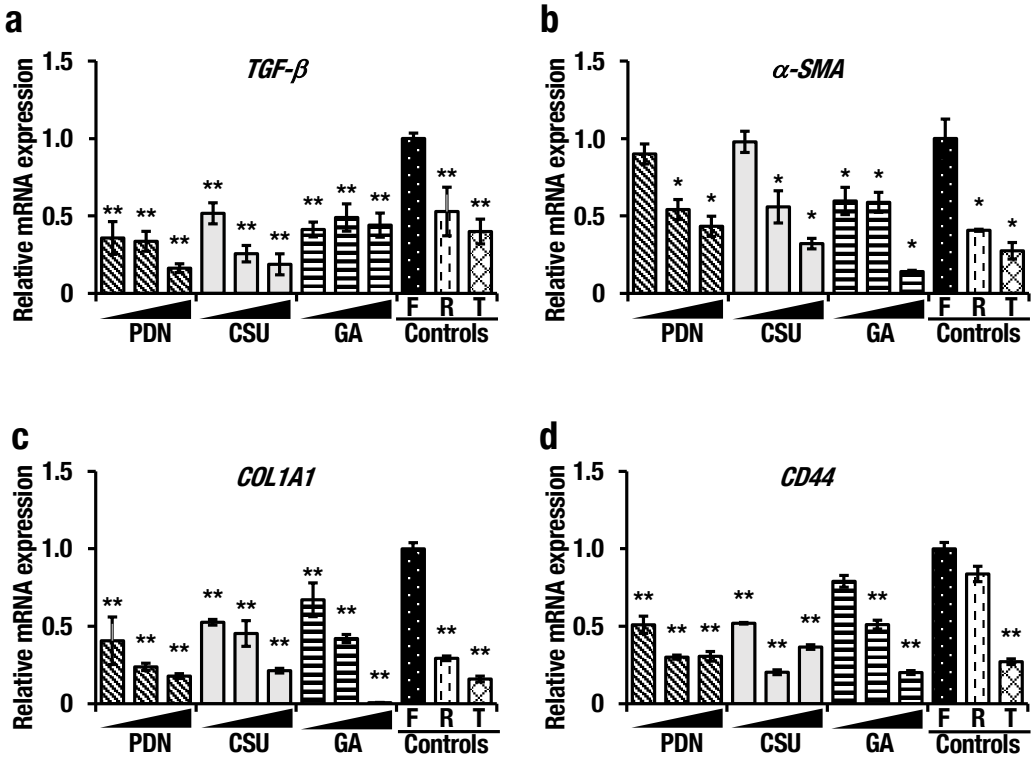

Figure 4-7: Pedunculagin, casuarinin and gallic acid mediate fibrosis via downregulating the mRNA expression levels of key fibrotic markers. (a-d) mRNA expression levels of key fibro genetic markers, *TGF-β* (a), *α-SMA* (b), *COL1A1* (c), and *CD44* (d) were measured with RT-qPCR after treatment with different concentrations (25, 50 and 100 μM) of different isolated compounds and controls (fibrosis induced group (control F); treated with 10% FBS only, gradually recovered group (control R); treated with 2% FBS and treatment positive group (control T); treated with 5 μM of doxorubicin) for 24 hours in activated LX-2 cells. Expression levels are normalized to *18S* rRNA level. Data based on the value from control F set as 1.0. **p* <0.05, ***p* <0.01 (one way ANOVA with Dunnett's test). Each data is mean ± SD (n=3).

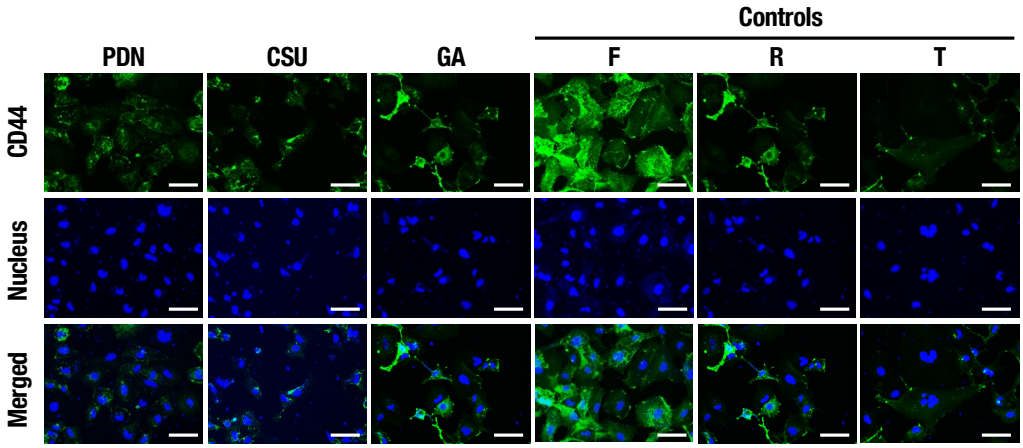

Figure 4-8: Pedunculagin, casuarinin and gallic acid mediate fibrosis via down regulation of CD44 expression. Immunohistochemistry analyses of CD44: activated LX-2 cells were treated with 50 μM of different isolated compounds and controls (fibrosis induced group (control F); treated with 10% FBS only, gradually recovered group (control R); treated with 2% FBS and treatment positive group (control T); treated with 5 μM of doxorubicin) for 24 hours in activated LX-2 cells. In the first raw, CD44 expression is shown in green. In the second raw, nuclear staining with DAPI shown in blue. In the third raw, both CD44 and DAPI merged images are shown. All images were taken at 200× magnification. Scale bar=50 μm.

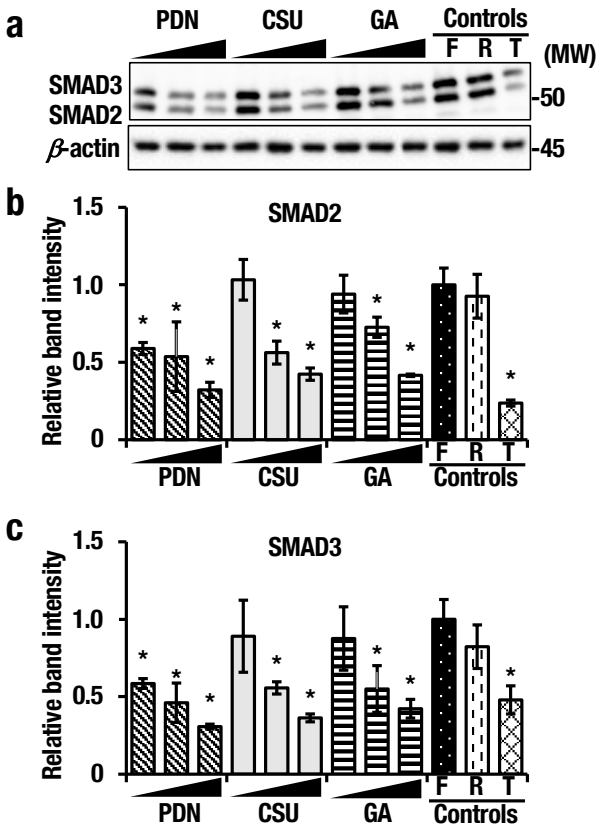

Figure 4-9: Pedunculagin, casuarinin and gallic acid mediate fibrosis via regulation of SMAD protein expression. (a) Immunoblot analyses of SMAD2 and SMAD3: activated LX-2 cells were treated with different concentrations (25, 50 and 100 μM) of different isolated compounds and controls (fibrosis induced group (control F); treated with 10% FBS only, gradually recovered group (control R); treated with 2% FBS and treatment positive group (control T); treated with 5 μM of doxorubicin) for 24 hours. Equal loading was sassed by probing the blots with antibody against *β*-actin. (b - c) Relative band intensity of SMAD2 (b) and SMAD3 (c). Band intensities were measured with image J software. Data based on the value from control F set as 1.0. **p* <0.05, ***p* <0.01 (one way ANOVA with Dunnett's test). Each data is mean ± SD (n=3).

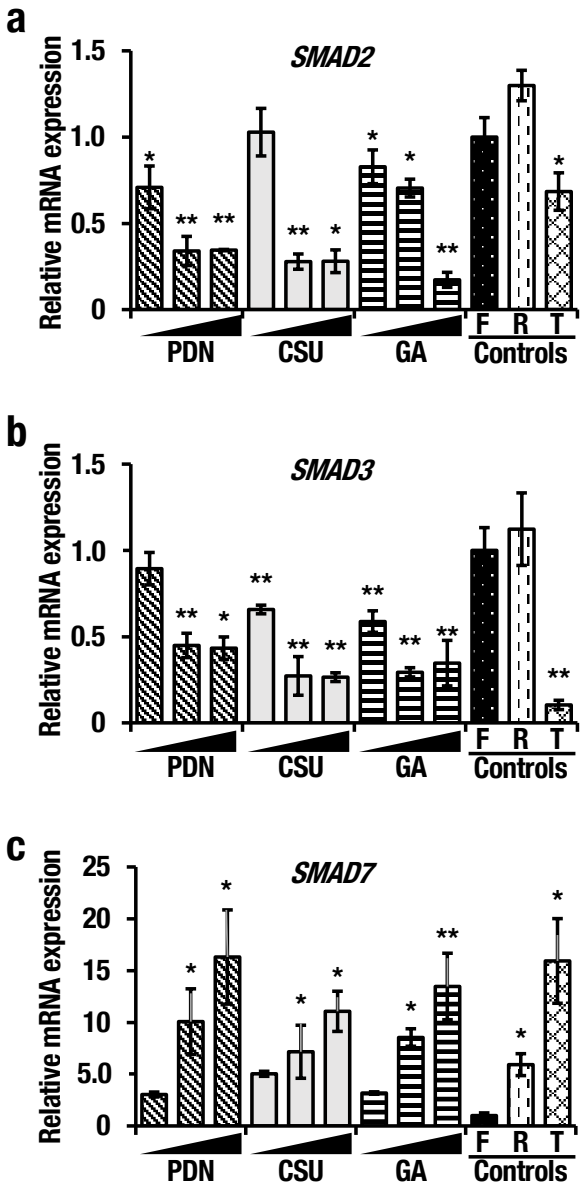

Figure 4-10: Pedunculagin, casuarinin and gallic acid mediate fibrosis via regulation of SMAD mRNA expression. (a-c) mRNA expression levels of *SMAD2* (a), *SMAD3* (b), and *SMAD7* (c) were measured by RT-qPCR after treatment with various concentrations (25, 50 and 100 μM) of different isolated compounds and controls (fibrosis induced group (control F); treated with 10% FBS only, gradually recovered group (control R); treated with 2% FBS and treatment positive group (control T); treated with 5 μM of doxorubicin) for 24 hours in activated LX-2 cells. Expression levels are normalized to *18S* rRNA level. Data based on the value from control F set as 1.0. **p* <0.05, ***p* <0.01(one way ANOVA with Dunnett's test). Each data is mean ± SD (n=3).

CHAPTER 05

Pedunculagin, Casuarinin and Gallic acid ameliorate fibrosis through mediating oxidative stress and ER stress in hepatic stellate cells (HSCs)

5-1. Introduction

In previous chapter we identified three major bio active compounds which poses antifibrotic effect. There is growing evidence that targeting oxidative stress and endoplasmic reticulum (ER) stress may be a promising therapeutic strategy for ameliorating liver fibrosis. Oxidative stress is known to play a critical role in the development and progression of liver fibrosis, and emerging evidence suggests that oxidative stress can induce ER stress in hepatic stellate cells (HSCs), promoting fibrosis.

Oxidative stress can induce ER stress in HSCs through several mechanisms. First, reactive oxygen species (ROS) generated by oxidative stress can directly damage ER-resident proteins, such as chaperones and enzymes involved in protein folding, leading to the accumulation of unfolded or misfolded proteins in the ER and triggering the unfolded protein response (UPR). Second, oxidative stress can disrupt ER redox balance, which is crucial for proper protein folding and assembly. Disruption of ER redox balance can lead to the accumulation of misfolded proteins and activation of the UPR. Third, oxidative stress can induce lipid peroxidation, which can lead to the formation of reactive aldehydes, such as 4-hydroxynonenal (4-HNE). 4-HNE can modify ER-resident proteins, leading to protein misfolding and activation of the UPR. Once ER stress is activated, it can promote fibrosis by inducing the expression of profibrotic genes and activating signaling pathways that promote fibrosis. This chapter was aimed to study the effect of three ellagitannin how mediate fibrosis through mediating oxidative stress and ER stress in activated HSCs. Moreover, as an additional experiment mRNA expression of genes related to Wnt-/β-catenin signaling pathway, were studied.

5-2. Experimental Section

5-2-1. Isolation and identification of ellagitannins

Three ellagitannins were isolated and identified from *Osbeckia octandra* as described previously.

5-2-2. Detection of reactive oxygen species (ROS)

Oxidative stress caused by isolated compound in activated LX-2 cells were shown qualitatively by fluorescent staining of the cells with ROS Assay kit – highly sensitive DCFH-DA (Invitrogen, Image-iT, I36007). Cells cultured on cover slips were washed with warm HBSS and covered with H_2 DCFH-DA working solution and incubated for 30 min at 37ºC in the dark. Thereafter, cells were washed three times with HBSS and nuclei were counterstained with 0.1 mg/mL of DAPI (4 -6-diamidino-2-phenylindole, Sigma- Aldrich, D9564) for 1min and washed.

5-2-3. Immunoblot analysis

The LX-2 cells (5.0×10^5 cells/well) were seeded in a 12-well plate and cultured in 10% FBS for 24 hours. The medium was then replaced with a fresh medium containing different concentrations of *O. octandra* fractions or isolated compounds and stimulated for 24 hours. After stimulation, the cells were lysed with sodium dodecyl sulphate (SDS) sample buffer (125 mM Tris-HCl, pH 6.8, 100 mM DTT, 2% [w/v] SDS, 5% [w/v] sucrose, 0.002% [w/v] bromophenol blue), centrifuged at 13000 rpm for 5 min, and boiled at 90 °C for 5 min. The sam- ples were subjected to SDS-polyacrylamide gel electrophoresis and transferred to polyvinylidene fluoride membranes (Fujifilm Wako). The membranes were blocked and incubated with primary antibodies against Binding immunoglobulin protein (BiP), Activating transcription factor 6 (ATF-6), PKR-like ER kinase (PERK) and inositol-requiring enzyme 1 α (IRE1-α) Tumor protein p53 (p53), β-catenin (Cell Signal Technology, Danvers, MA, USA), or *β*-actin (Fujifilm Wako). The membranes were then washed and incubated with horseradish

peroxidase (HRP)-conjugated secondary antibodies. Signals were detected with ImmunoStar LD (Fujifilm Wako) using Lumino Graph I (ATTO, Tokyo, Japan).

5-2-4. RNA isolation and quantitative PCR

mRNA expression analysis was one as described in previously for *Wnt-1*. *Wnt-3*, *Fibronectin*, *IL-1*, *c-Myc*, *Cyclin D1*, *TNF-α* and *GSK3-β*. The primers used for this study are listed in Table 5-1. The 18S rRNA expression was used as an internal control to normalize the mRNA expression data.

5-2-5. Statistical analysis

Statistical analyses were performed by one-way analysis of variance (ANOVA) with a Dunnett test. All data were expressed as mean ± standard error of the mean (mean ± SEM).

5-3. Results

5-3-1. Pedunculagin, Casuarinin and Gallic Acid showed therapeutic effect via regulation of oxidative stress.

Studies have shown that oxidative stress damage was related to liver fibrosis. To determine whether PDN, CSU and GA inhibits oxidative-stress-induced ROS production in activated LX-2 cells, DCFDA dye, an ROS detector, staining was performed in cells. The results showed that intracellular ROS production detected by green fluorescence was markedly increased in positive control. However, treatment with PDN, CSU and GA significantly inhibited ROS production in dose dependent manner. This ROS production indicate the reduction of oxidative stress in activated HSCs confirming the reversion from activated state to quiescent state in line with negative control which is treated with 2% FBS (Fig.5-1).

5-3-2. Pedunculagin, Casuarinin and Gallic Acid showed therapeutic effect via regulation of Endoplasmic Reticulum stress signaling pathway.

Activation of HSCs contribute the to the development ER stress which induces fibro genetic genes and promotes fibrosis. To study weather PDN, CSU and GA can suppress fibrosis by regulating ER stress, we measured the protein levels of Bip, the central regulator of ER stress and three ER stress sensors (IRE1-α, PERK and ATF-6) (Fig.5-2A). Interestingly, we observed compared to the positive control, PDN treatment significantly reduced Bip expression in dose dependent manner. CSU treatment significantly down regulated Bip expression in medium (50 μM) and high (100 μM) doses but not with the low dose. Further, GA significantly down regulated Bip expression only in and high (100 μM) dose. Here we could not observe any significant different between three controls (Fig. 5-2B). ATF-6 is significantly down regulated with the treatment of PDN, protein band is mealy in visible. CSU treatment also significantly reduced the ATF-6 expression level in line with both negative and standard control. GA treatment showed significant down regulation of ATF-6 expression which is dose dependent

(Fig. 5-2C). PERK is down regulated by PDN and CSU in dose dependent manner while GA showed significant down regulation in medium (50 μM) and high (100 μM) doses only which is compatible with negative and standard controls (Fig. 5-2D). IRE1-α is significantly down regulated only with PDN treatment in medium (50 μM) and high (100 μM) doses. There is no significant difference of IRE1-α with the treatment of CSU compared to positive control. Low and medium doses of GA significantly increased the IRE1-α expression compared to positive control. Negative control also not significantly different with positive control but standard control is significantly down regulated IRE1-α protein expression (Fig. 5-2E).

5-3-3. Pedunculagin, Casuarinin and Gallic Acid showed therapeutic effect via regulation of Wnt/β-catenin signaling pathway

Another highly conserved transduction pathway known to be involved in several important biological processes, such as liver development, vascular and hepatic differentiation, and tissue homeostasis is the Wnt-/β-catenin signaling pathway. To understand the contribution of this signaling pathway in reversing fibrosis in LX-2 cells by PDN, CSU and GA, expression of p53, β-catenin and Wnt target genes were studied. p53 protein expression levels were significantly down regulated by PDN, CSU and GA in medium (50 μM) and high (100 μM) doses but not in the low dose (25 μM). However, there is no significant difference between positive control and negative control, but standard control is significantly down regulated p53 protein expression compared to positive control. β-catenin protein expression levels were significantly up regulated in low and medium doses with the treatment of PDN and CSU. Treatment with low dose of GA significantly upregulated β-catenin protein expression. Both positive and negative control significantly down regulated β-catenin protein expression compared to positive control.

To understand the gene expressions of p53 and β-catenin, which is responsible for the therapeutic effect, mRNA expression expressions were studied. Interestingly, PDN, CSU and GA treatment significantly reduced p53 expression. Moreover, negative control and standard control also significantly down regulated p53 mRNA expression compared to positive control. As expected, β-catenin mRNA expression significantly upregulated with the treatment of PDN, CSU and GA. Even though, negative control significantly up regulated β-catenin expression level compared to positive control, standard control is not significantly upregulated.

To further understand the Wnt behavior and its target genes, mRNA expression of relevant genes were studied. Relative mRNA expressions of Wnt-1 and Wnt-3 were significantly down regulated with the treatment of PDN, CSU and GA. In the same time bot negative control and standard control also significantly down regulated Wnt gene expressions compared to the positive control. These results suggest PDN, CSU and GA contributed for the down regulation of Wnt signals while reversing fibrosis.

To further confirm this down regulation mRNA expression of relevant genes were studied. Fibronectin was significantly down regulated in dose dependent manner in PDN, CSU and GA. Negative control also showed significant down regulation compared to positive control but not with the standard control. c-Myc and IL-1 mRNA expressions were significantly down regulated in all treated groups compared to positive control. mRNA expression level of cyclin-D1 also significantly down regulated with the treatment of PDN, CSU and GA (except high dose) and standard control. However negative control and high dose in GA treatment significantly up regulated cyclin-D1 mRNA expression compared to positive control.

5-4. Discussion

An increasing number of studies support the view that ER stress is associated with the pathogenesis of liver diseases and hepatic fibrosis through the activation of unfolded protein response (UPR) in hepatocytes and HSCs [75]. Upon HSCs activation in response to a potent inducer, ER stress was noted in these studies. UPR activation also causes fibrogenesis in HSCs and therefore ER stress may be a driver of HSCs activation. These observations show that ER stress plays a crucial role in HSC activation as well as liver fibrosis. Activated HSCs increased secretory load and drive the cell's protein synthesis needs beyond what the capacity of the ER could cope with to ensure accurate protein folding. In these situations, three conserved ER transmembrane sensory proteins known as inositol-requiring enzyme 1α (IRE1-α), protein kinase RNA-like ER kinase (PERK) and transmit alarm signals to the nucleus and cytosol to restore protein-folding capacity, which aims to restore normal ER function and homeostasis [76]. In non-stressed cells, these three UPR signaling transducers remain inactive and anchored to the ER membrane through binding to BiP (Bip also known as GRP78, is a master regulator of unfolded protein response in ER) with their luminal domains [77]. However, upon unfolded protein accumulation in the ER lumen, BiP dissociates from the UPR transducers, releasing their luminal domains and allowing for their subsequent activation [78]. Our study presented that ER stress in activated HSCs, is ameliorated by PDN, CSU and GA via down regulating Bip, ATF-6, PERK and IRE1-α. Notably, PDN and CSU mediate ER stress via downregulating ATF-6 massively while PERK and IRE1-α in dose dependent manner. This kind of down regulation could be observed with the treatment of celastrol in palmitate induced ER stress [79]. However, with the treatment of GA expression of IRE1-α not downregulated.

p53 is a well-known tumor suppressor gene and recent studies revealed that p53 also plays an important role in the development and progression of fibrosis [80]. p53 is an upstream molecule that promotes artemether-induced ferroptosis in HSCs and inhibits HSCs activation

accordingly [80]. This phenomenon was confirmed in our study by significantly downregulating markers of HSCs activation, including α-SMA and COL1A1 as well as and inhibiting profibrotic marker such as TGF-*β*. These results are in line with the previously reported in the ferroptosis induced antifibrotic study [81]. Here we observed downregulation of β-catenin and upregulation of p53 with the treatment of PDN, CSU and GA in activated HSCs. Activated p53 can feed back and downregulate β-catenin expression.

β-catenin is a protein with dual functions, acting as both an adhesion molecule and a transcription factor. The functions of β-catenin as a transcription factor are mainly regulated by Wnt proteins [82]. In normal cells, β-catenin is evident in the cytoplasm (total β-catenin) and nucleus (active β-catenin) to regulate target factors and activate target genes in the Wnt pathway. With the onset of fibrosis, the total β-catenin, which accumulated in the cytoplasm, could enter the nucleus as its active form, known as the active β-catenin, and then combined with lymphocyte factor/lymphotropic factor (LEF/TCF), which can activate target genes of the Wnt signaling pathway, increasing pro-fibro genic cytokines and protein expression of EMC compounds in fibrogenesis. The TGF/β-catenin complex binds DNA and promotes the transcription of Wnt target genes, such as cyclin D1, c-Myc, IL-1 and fibronectin [83]. This phenomenon was in line with our positive control in activated LX-2 cell culture model. However, with the treatment of PDN, CSU and GA. Wnt signaling is inactivated and significantly down regulated the expressions of Wnt target genes while upregulating GSK3-β. This may be due to the phosphorylation of β-catenin by GSK3-β and the promotion its subsequent proteasomal degradation in response to the above-described compounds, which are present in *O.ocatndra*. Furthermore, these findings support the fact that PDN, CSU and GA act as Wnt/β-catenin inhibitors, indicating their potential as therapeutic options for liver fibrosis.

Table 5-1: Primers used for qPCR in this *chapter*

Gene	Sequence
Human-WNT-1	F; 5′–CCTCCACGAACCTGCTTACA–3′ R; 5′–TCCCCGGATTTTGGCGTATC–3′
Human-WNT-3	F; 5′–TGGAGCAGGACTCCCACCTA–3′ R; 5′–GCCACCAGAGAGGAGACACTA–3′
Human-Fibronectin	F; 5′–CCATCGCAA ACCGCTGCCAT–3′ R; 5′–AACACTTCTCAGCTATGGGCTT–3′
Human-IL-1	F; 5′–GATCGGTGGCTCCATCCT–3′ R; 5′–CGGCTTCATCGTATTCCTGTT–3′
Human-cMyc	F; 5′–ATCCCTAACTCTACATCAACCC–3′ R; 5′–TTCAAATCTCGCTTCCACTT–3′
Human-Cyclin D1	F; 5′–GCATCTACACCGACAACTCC–3′ R; 5′–GATGATCTGTTTGTTCTCCTCC–3′
Human-TNF-α	F; 5′–CTCGGACAGCTCAATTCGGA–3′ R; 5′–CAGTGTGGCGGACTTGATGA–3′
Human-GSK3-β	F; 5′–TACCTGAACCCGTGTTGCTCTC–3′ R; 5′–GTTGCTGAGGTATCGCCAGGAA–3′
Human-18S	F; 5′–GTAACCCGTTGAACCCCATT–3′ R; 5′–CCATCCAATCGGTAGTAGCG–3′

[a] F; forward primer. [b] R; Reverse primer.

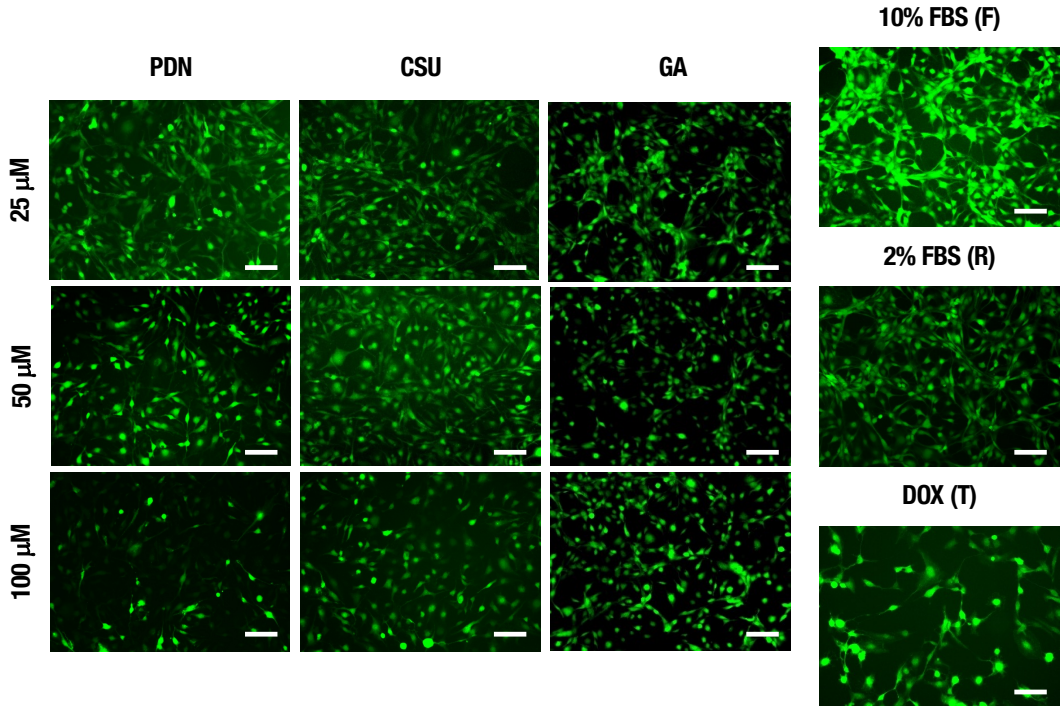

Figure 5-1: Pedunculagin, casuarinin and gallic acid mediate fibrosis via Oxidative stress. Detection of ROS using DCF DA dye, visualize in green florescent: activated LX-2 cells were treated with 25, 50, 100 µM of different isolated compounds. First and second raw shows PDN and CSU reduce ROS generation in dose dependent manner compared to GA. Right side column shows controls (fibrosis induced group (control F); treated with 10% FBS only, gradually recovered group (control R); treated with 2% FBS and treatment positive group (control T); treated with 5 µM of doxorubicin) for 24 hours. All images were taken at 100× magnification. bar=20 µm.

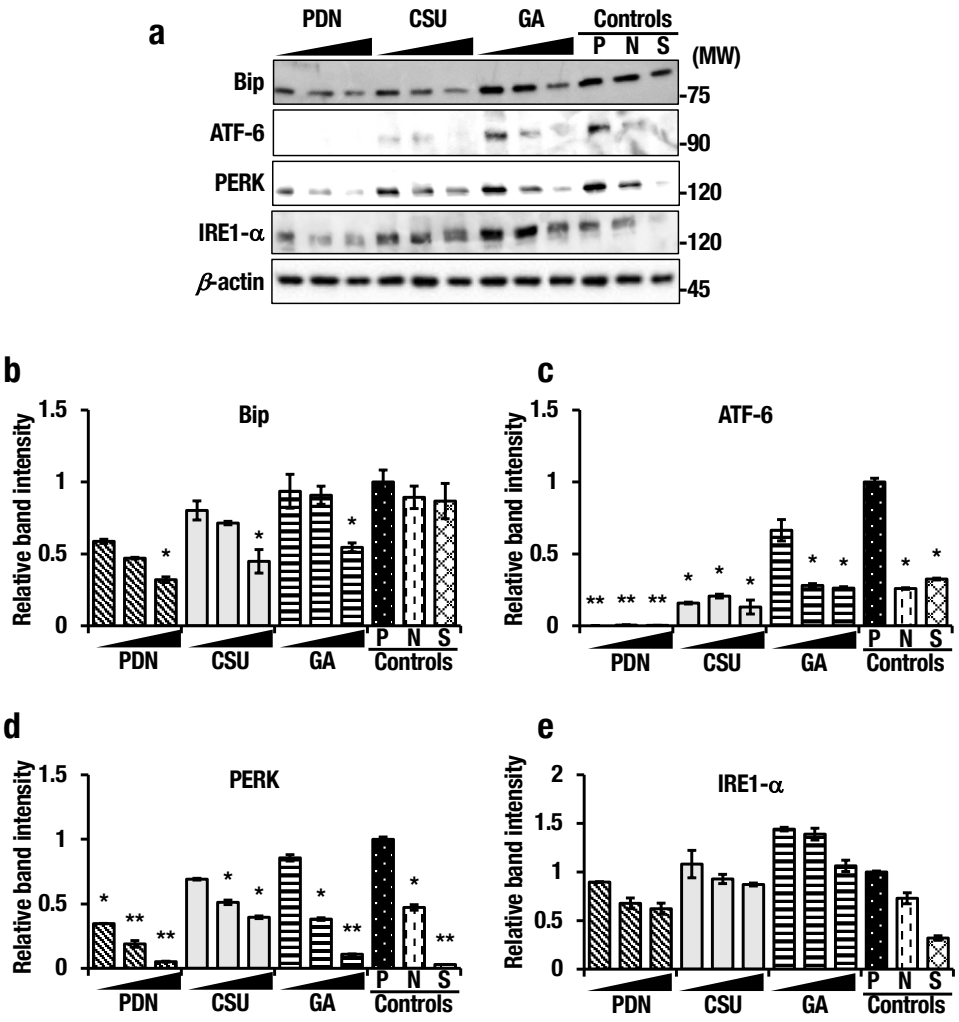

Figure 5-2: Pedunculagin, casuarinin and gallic acid mediate fibrosis via regulation of ER stress sensors. a) Immunoblot analyses of Bip, ATF-6, PERK and IRE1-α. Activated LX-2 cells were treated with different concentrations (25, 50 and 100 μM) of different isolated compounds and controls (fibrosis induced group (control P); treated with 10% FBS only, gradually recovered group (control N); treated with 2% FBS and treatment positive group (control S); treated with 5 μM of doxorubicin) for 24 hours. Equal loading was sassed by probing the blots with antibody against β-actin. (b - c) Relative band intensity of Bip (b) and ATF-6 (c), PERK (d) and IRE1-α (e). Band intensities were measured with image J software. Data based on the value from control F set as 1.0. (one way ANOVA with Dunnett's test). Each data is mean ± SD (n=3).

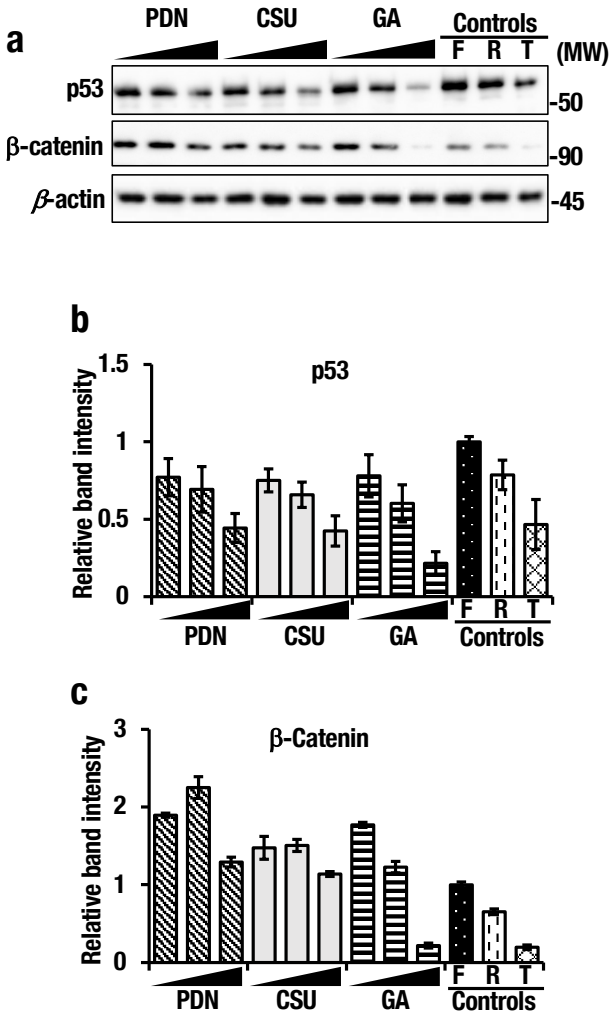

Figure 5-3: Effect of Pedunculagin, casuarinin and gallic acid on β-catenin regulation pathway. a) Immunoblot analyses of p53 and β-catenin. Activated LX-2 cells were treated with different concentrations (25, 50 and 100 μM) of different isolated compounds and controls (fibrosis induced group (control F); treated with 10% FBS only, gradually recovered group (control R); treated with 2% FBS and treatment positive group (control T); treated with 5 μM of doxorubicin) for 24 hours. Equal loading was sassed by probing the blots with antibody against *β*-actin. Relative band intensity of p53 (b) and β-Catenin (c). Band intensities were measured with image J software. Data based on the value from control F set as 1.0. Each data is mean ± SD (n=3).

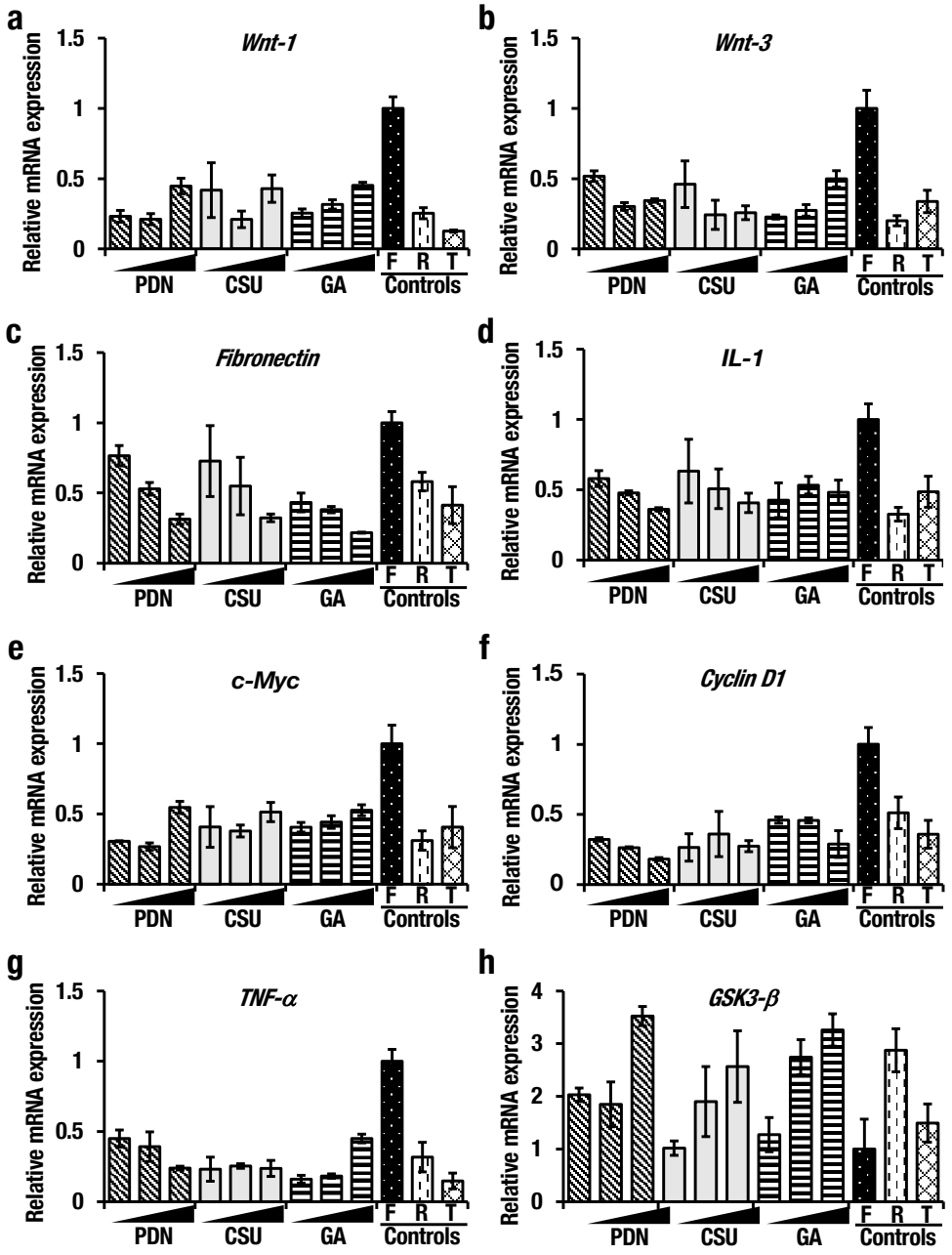

Figure 5-4: Effect of Pedunculagin, casuarinin and gallic acid on Wnt target genes. (a-h) mRNA expression levels of Wnt-1, Wnt-2, Fibronectin, IL-1, c-Myc, Cyclin D-1, TNF-α and GSK3-β were measured by RT-qPCR after treatment with various concentrations (25, 50 and 100 μM) of different isolated compounds and controls controls (fibrosis induced group (control F); treated with 10% FBS only, gradually recovered group (control R); treated with 2% FBS and treatment positive group (control T); treated with 5 μM of doxorubicin) for 24 hours in activated LX-2 cells. Expression levels are normalized to *18S* rRNA level. Data based on the value from control F set as 1.0. Each data is mean ± SD (n=3).

CHAPTER 06
General Discussion

Liver fibrosis, cirrhosis, and the progression to liver carcinoma cause significant morbidity and mortality worldwide [22]. Currently, there is limited treatment option available for advanced liver fibrosis and cirrhosis in humans, with liver transplantation being the most viable option for cirrhotic patients. Synthetic drugs like doxorubicin, metformin, silymarin, colchicines, penicillamine, and corticosteroids are used to treat chronic liver diseases [8,9] but their effectiveness is limited and they can have adverse side effects. Treating liver diseases with plant compounds is a cost-effective and relatively safe approach, as these herbs can be used for both treatment and prevention of liver diseases [15].

In this study, our focus was on investigating the potential benefits of *O. octandra*, an herbal plant commonly used in Sri Lanka for various ailments. Specifically, we examined the effects of the boiled water extract (BLE) derived from this plant. Our findings revealed that the BLE of *O. octandra* holds promise as both a preventive measure and a therapeutic intervention for fibrosis. Despite several studies conducted to assess the potential health benefits of *O. octandra*, these studies have primarily utilized crude extracts of the plant.

There is currently no available information regarding the isolation of specific compounds from *O. octandra*. To identify the major active compounds present in the extract of *O. octandra*, we conducted extract fractionation and isolation procedures as outlined in Chapter 3 of our study. As described in the chapter 4 here we established a cell culture model using LX-2 cells, a cell lined derived from human HSCs. This cell culture model allows to identify antifibrotic compound effectively.

The isolated compounds were subsequently identified using advanced techniques such as Nuclear Magnetic Resonance (NMR) and Gas Chromatography-Mass Spectrometry (GC-MS).

Isolated compounds were identified as pedunculagin (PDN), casuarinin (CSU), and gallic acid (GA), which are polyphenols in the group of hydrolysable tannins. They can further be classified into gallo tannin (GA) and ellagitannin (PDN and CSU) [55]. The ellagitannins, although present in red wine, oak, chestnut, raspberry, and pomegranate, have received little attention as potential bioactive compounds [55]. According to the phytochemical analysis, PDN, CSU, and GA are found in the dry leaves of *O. octandra* in amounts of 0.02%, 0.12%, and 0.04%, respectively. The ellagitannins, although present in red wine, oak, chestnut, raspberry, and pomegranate, have received little attention as potential bioactive compounds [84].

In Chapter 4 of our study, we conducted experiments to confirm the fibrosis effect of the isolated compounds. Through these experiments, we identified that one of the regulatory pathways involved in the regulation of fibrosis is the TGF-β/SMAD pathway. This pathway plays a crucial role in the development and progression of fibrosis and cirrhosis. By elucidating the involvement of this pathway, we gained valuable insights into the molecular mechanisms underlying the observed effects of the isolated compounds on fibrosis and cirrhosis.

In Chapter 5 of our study, we conducted additional experiments to further understand the regulatory mechanisms related to fibrosis. Our focus shifted towards investigating oxidative stress and ER stress, both of which play significant roles in the development and progression of fibrosis. By examining these mechanisms, we aimed to gain a more comprehensive understanding of the molecular pathways involved in fibrosis. These experiments allowed us to explore the impact of oxidative stress and ER stress on fibrosis development and provided valuable insights into the underlying mechanisms contributing to this condition. However additional experiments are needed to fully understand those mechanism related to intervention for the fibrosis signaling.

In addition, as a sub-experiment, we specifically focused on the β-catenin pathway, as it plays a crucial role in the regulation of fibrosis. We investigated the effects of the isolated compounds on key factors involved in this pathway, such as p53 and β-catenin. Through our experiments, we observed significant changes in the expression or activity of these factors upon treatment with the isolated compounds. This provided further evidence of the regulatory effects of the compounds on the β-catenin pathway, shedding light on their potential mechanisms of action in mitigating fibrosis. Together with these sub studies, it is important do in-depth analysis such as RNA sequencing analysis or proteomics analysis to understand the responsible pathways which intervene by *O. octandra*.

In this study, we focused only on three major compounds; PDN, CSU and GA which present in *O. octandra* which were found in the dry leaves of *O. octandra*, at levels of 0.143, 0.310, and 0.012% respectively. There may be another antifibrotic compound(s) responsible for the antifibrotic effect. Future experiments will be carried out to identify another possible compound(s) present in *O. ocatndra*.

Moreover, our study revealed that *O. octandra* exerts its antifibrotic effects through various regulation pathways. In addition to the previously mentioned pathways, there may be other hidden regulatory pathways involved. Advanced experiments are necessary to explore and uncover any hidden regulatory pathways that may contribute to the antifibrotic properties of *O. octandra*. By conducting these comprehensive investigations, we can gain a more thorough understanding of the compound profile and the multiple regulation pathways involved in the antifibrotic effects of *O. octandra*. This knowledge will contribute to the development of effective therapeutic strategies for treating fibrosis. In addition, its therapeutic potential to interfere with fibrotic progression in kidney, lung, pancreas and stomach and to reduce chronic inflammatory status will be investigated.

Acknowledgement

I would like to express my deepest gratitude and appreciation to Ministry of Education, Culture, Sports, Science and Technology (Monbukagakusho (MEXT)) for providing me with the opportunity to pursue my doctoral studies.

I am extremely grateful to my supervisor, Associate Professor Tadayuki Tsujita, for giving this unevaluable opportunity to pursue my research in his laboratory as a PhD student and his guidance, expertise, and unwavering support throughout this journey. His mentorship, encouragement, and constructive feedback have been instrumental in shaping my research and pushing me to reach new heights.

I would like to acknowledge the assistance and cooperation received from Professor Kanji Ishimaru and Professor Shin-ichi Kawaguchi along with their research team who have contributed to fruitful collaborations.

I would like to express my deep appreciation to laboratory members and all the participants who willingly took part in my research. Their willingness to contribute their time and knowledge has been fundamental in the completion of this study.

I am grateful to the faculty and staff of Saga University and Kagoshima University, who have provided a conducive academic environment and access to necessary resources, libraries, and laboratories that were essential for conducting my research accomplishments.

References

1. Metcalf J. Functional anatomy and blood supply of the liver. *Anaesth Intensive Care Med*. 2011;13(2):52-53. doi:10.1016/j.mpaic.2011.11.005

2. Schuppan D, Afdhal NH, Israel B. Liver cirrhosis. *Lancet*. 2008;371(9615):838-851. doi:10.1016/S0140-6736(08)60383-9

3. Juza RM, Pauli EM. Clinical and surgical anatomy of the liver: A review for clinicians. *Clin Anat*. 2014;27(5):764-769. doi:10.1002/ca.22350

4. Murase K, Morrison KL, Tam PY, Stafford RL, Jurnak F, Weiss GA. EF-Tu Binding Peptides Identified, Dissected, and Affinity Optimized by Phage Display. *Chem Biol*. 2003;10(2):161-168. doi:10.1016/S1074-5521(03)00025-5

5. Chen D, Le TH, Shahidipour H, Read SA, Ahlenstiel G. The role of gut-derived microbial antigens on liver fibrosis initiation and progression. *Cells*. 2019;8(11):55-64. doi:10.3390/cells8111324

6. Wong SW, Ting YW, Chan WK. Epidemiology of non-alcoholic fatty liver disease-related hepatocellular carcinoma and its implications. *JGH Open*. 2018;2(5):235-241. doi:10.1002/jgh3.12070

7. Wang FS, Fan JG, Zhang Z, Gao B, Wang HY. The global burden of liver disease: The major impact of China. *Hepatology*. 2014;60(6):2099-2108. doi:10.1002/hep.27406

8. Greupink R, Bakker HI, Bouma W, et al. The antiproliferative drug doxorubicin inhibits liver fibrosis in bile duct-ligated rats and can be selectively delivered to hepatic stellate cells in vivo. *J Pharmacol Exp Ther*. 2006;317(2):514-521. doi:10.1124/jpet.105.099499

9. Lavine JE, Schwimmer JB, Van Natta ML, et al. Effect of Vitamin e or metformin for

treatment of nonalcoholic fatty liver disease in children and adolescents the tonic randomized controlled trial. *Jama*. 2011;305(16):1659-1668. doi:10.1001/jama.2011.520

10. Freedman ND, Curto TM, Morishima C, et al. Silymarin use and liver disease progression in the Hepatitis C Antiviral Long-Term Treatment against Cirrhosis trial. *Aliment Pharmacol Ther*. 2011;33(1):127-137. doi:10.1111/j.1365-2036.2010.04503.x

11. Jayathilaka KAPW, Thabrew MI, Pathirana C, De Silva DGH, Perera DJB. An evaluation of the potency of Osbeckia octandra and Melothria maderaspantana as antihepatotoxic agents. *Planta Med*. 1989;55(2):137-139. doi:10.1055/s-2006-961906

12. Ravi S, Sujini R. ANTIMICROBIAL AND CYTOTOXIC ACTIVITIES SCREENING OF SOME MEDICINAL PLANTS. *Int J Compr Lead Res Sci*. 2016;2(3):11-21.

13. Saleem TSM, Chetty CM, Ramkanth S, Rajan VST, Kumar KM, Gauthaman K. Hepatoprotective Herbs- A Review. *Int J Res Pharm Sci*. 2010;1(1):1-5.

14. Wijayagunawardane MPB, Wijerathne CUB, Herath CB. Indigenous Herbal Recipes for Treatment of Liver Cirrhosis. *Procedia Chem*. 2015;14(1):270-276. doi:10.1016/j.proche.2015.03.038

15. Sahar S. Atrees HMR. Herbs and Supplements for Liver Toxicity: A Review on Mode of Action of Herbs and Supplements on Liver Toxicity. *Med J Cairo Univ*. 2021;89(9):2179-2183. doi:10.21608/mjcu.2021.203687

16. Zhang A, Sun H, Wang X. Recent advances in natural products from plants for treatment of liver diseases. *Eur J Med Chem*. 2013;63:570-577. doi:10.1016/j.ejmech.2012.12.062

17. Thabrew MI, Hughes RD, Gove CD, Portmann B, Williams R, McFarlane IG. Protective effects of Osbeckia octandra against paracetamol-induced liver injury. *Xenobiotica*. 1995;25(9):1009-1017. doi:10.3109/00498259509046671

18. Anuruddhika Subhashinie Senadheera SP, Ekanayake S. Green leafy porridges: How good are they in controlling glycaemic response? *Int J Food Sci Nutr*. 2013;64(2):169-174. doi:10.3109/09637486.2012.710895

19. Prasanna KD, Gunathilake P, Gunathilake KDPP, Gam Lath GGS. *Development of Instant Herbal Porridge Mixtures from Osbeckia Octandra Leaves Development of Instant Herbal Porridge Mixtures from Heenbowitiya (Osbeckia Octandra L.) Leaves*. Vol 14.; 2002. https://www.researchgate.net/publication/256765971

20. Prasadani M, Bogahawaththa S, Illeperuma RP, Kodithuwakku SP. Leaf Extract of Osbeckia octandra L. (Heen Bovitiya) Suppresses Human Oral Squamous Cell Carcinoma Cells Migration and Induces Cellular DNA Damage. *J Oral Maxillofac Surgery, Med Pathol*. 2021;33(2):215-220. doi:10.1016/j.ajoms.2020.09.003

21. Grayer RJ, Thabrew MI, Hughes RD, et al. Phenolic and terpenoid constituents from the Sri Lankan medicinal plant Osbeckia aspera. *Pharm Biol*. 2008;46(3):154-161. doi:10.1080/13880200701538682

22. Golabi P, Paik JM, Eberly K, de Avila L, Alqahtani SA, Younossi ZM. Causes of death in patients with Non-alcoholic Fatty Liver Disease (NAFLD), alcoholic liver disease and chronic viral Hepatitis B and C. *Ann Hepatol*. 2022;27(1):100556. doi:10.1016/j.aohep.2021.100556

23. Jaeschke H, Farhood A, Smith CW. Neutrophils contribute to ischemia/reperfusion injury in rat liver in vivo. *FASEB J*. 1990;4(15):3355-3359. doi:10.1096/fasebj.4.15.2253850

24. Mailliard ME, Gollan JL. Emerging therapeutics for chronic hepatitis B. *Annu Rev Med*. 2006;57(5):155-166. doi:10.1146/annurev.med.57.121304.131422

25. Tsochatzis EA, Bosch J, Burroughs AK. Liver cirrhosis. *Lancet*. 2014;383(9930):1749-

1761. doi:10.1016/S0140-6736(14)60121-5

26. Wijesundera KK, Izawa T, Tennakoon AH, et al. Experimental and Toxicologic Pathology M1- / M2-macrophages contribute to the development of GST-P -positive preneoplastic lesions in chemically-induced rat cirrhosis. *Exp Toxicol Pathol*. 2015;67(9):467-475. doi:10.1016/j.etp.2015.05.002

27. Yogalakshmi B, Viswanathan P, Anuradha CV. Investigation of antioxidant, anti-inflammatory and DNA-protective properties of eugenol in thioacetamide-induced liver injury in rats. *Toxicology*. 2010;268(3):204-212. doi:10.1016/j.tox.2009.12.018

28. Al-attar AM, Shawush NA. Influence of olive and rosemary leaves extracts on chemically induced liver cirrhosis in male rats. *SAUDI J Biol Sci*. 2014;22(2):1-22. doi:10.1016/j.sjbs.2014.08.005

29. Bocca C, Novo E, Miglietta A, Parola M. Angiogenesis and Fibrogenesis in Chronic Liver Diseases. *Cell Mol Gastroenterol Hepatol*. 2015;1(5):477-488. doi:10.1016/j.jcmgh.2015.06.011

30. Nakamura M, Yamabe H, Osawa H, et al. Hypoxic conditions stimulate the production of angiogenin and vascular endothelial growth factor by human renal proximal tubular epithelial cells in culture. *Nephrol Dial Transplant*. 2006;21(6):1489-1495. doi:10.1093/ndt/gfl041

31. Huang Q, Gumireddy K, Schrier M, et al. The microRNAs miR-373 and miR-520c promote tumour invasion and metastasis. *Nat Cell Biol*. 2008;10(2):202-210. doi:10.1038/ncb1681

32. Ramaiah SK. A toxicologist guide to the diagnostic interpretation of hepatic biochemical parameters. *Food Chem Toxicol*. 2007;45(9):1551-1557. doi:10.1016/j.fct.2007.06.007

33. Georges PC, Hui JJ, Gombos Z, et al. Increased stiffness of the rat liver precedes matrix

deposition: Implications for fibrosis. *Am J Physiol - Gastrointest Liver Physiol*. 2007;293(6):1147-1154. doi:10.1152/ajpgi.00032.2007

34. Thabrew M, Joice P, Rajatissa W. A Comparative Study of the Efficacy of Pavetta indica and Osbeckia octandra in the Treatment of Liver Dysfunction. *Planta Med*. 1987;53(03):239-241. doi:10.1055/s-2006-962691

35. Bogahawaththa S, Kodithuwakku SP, Wijesundera KK, et al. Anti-Fibrotic and Anti-Angiogenic Activities of Osbeckia octandra Leaf Extracts in Thioacetamide-Induced Experimental Liver Cirrhosis. *Molecules*. 2021;26(16):4836. doi:10.3390/molecules26164836

36. Wong W-L, Abdulla MA, Chua K-H, Kuppusamy UR, Tan Y-S, Sabaratnam V. Hepatoprotective Effects of Panus giganteus (Berk.) Corner against Thioacetamide-(TAA-) Induced Liver Injury in Rats. *Evidence-Based Complement Altern Med*. 2012;2012:1-10. doi:10.1155/2012/170303

37. Rhiouani H, El-Hilaly J, Israili Z, Lyoussi B. Acute and sub-chronic toxicity of an aqueous extract of the leaves of Herniaria glabra in rodents. *J Ethnopharmacol*. 2008;118:378-386.

38. Dwivedi DK, Jena GB. Glibenclamide protects against thioacetamide-induced hepatic damage in Wistar rat: investigation on NLRP3, MMP-2, and stellate cell activation. *Naunyn Schmiedebergs Arch Pharmacol*. 2018;391(11):1257-1274. doi:10.1007/s00210-018-1540-2

39. Lebeaupin C, Vallée D, Hazari Y, Hetz C, Chevet E, Bailly-Maitre B. Endoplasmic reticulum stress signalling and the pathogenesis of non-alcoholic fatty liver disease. *J Hepatol*. 2018;69(4):927-947. doi:10.1016/j.jhep.2018.06.008

40. El Awdan SA, Abdel Rahman RF, Ibrahim HM, et al. Regression of fibrosis by

cilostazol in a rat model of thioacetamide-induced liver fibrosis: Up regulation of hepatic cAMP, and modulation of inflammatory, oxidative stress and apoptotic biomarkers. *PLoS One*. 2019;14(5):e0216301. doi:10.1371/journal.pone.0216301

41. Jantararussamee C, Rodniem S, Taweechotipatr M, Showpittapornchai U, Pradidarcheep W. Hepatoprotective Effect of Probiotic Lactic Acid Bacteria on Thioacetamide-Induced Liver Fibrosis in Rats. *Probiotics Antimicrob Proteins*. 2021;13(1):40-50. doi:10.1007/s12602-020-09663-6

42. Yang YM, Seki E. TNFα in Liver Fibrosis. *Curr Pathobiol Rep*. 2015;3(4):253-261. doi:10.1007/s40139-015-0093-z

43. Dewidar B, Meyer C, Dooley S, Meindl-Beinker N. Tgf-β in hepatic stellate cell activation and liver fibrogenesis—updated 2019. *Cells*. 2019;8(11):1-35. doi:10.3390/cells8111419

44. Cao D, Shamsan E, Jiang B, Fan H, Zhang Y, Dehwah MAS. Structural changes and expression of hepatic fibrosis-related proteins in coculture of Echinococcus multilocularis protoscoleces and human hepatic stellate cells. *Parasites and Vectors*. 2021;14(1):1-9. doi:10.1186/s13071-021-05037-1

45. Wijesundera KK, Izawa T, Tennakoon AH, et al. Experimental and Toxicologic Pathology M1- / M2-macrophages contribute to the development of GST-P -positive preneoplastic lesions in chemically-induced rat cirrhosis. *Exp Toxicol Pathol*. 2015;67:467-475. doi:10.1016/j.etp.2015.05.002

46. Abdel-Rahman RF, Fayed HM, Asaad GF, et al. The involvement of TGF-β1 /FAK/α-SMA pathway in the antifibrotic impact of rice bran oil on thioacetamide-induced liver fibrosis in rats. *PLoS One*. 2021;16(12):e0260130. doi:10.1371/journal.pone.0260130

47. Perera PR., Ekanayake S, Ranaweera KKD. Comparison of Antiglycation and

antioxidant potentials and total phenolic contents of decoctions from antidiabetic plants. *Procedia Chem*. 2015;16:519-524.

48. Thabrew MI, Jayatilaka KAPW. A comparative study of the beneficial effects of Osbeckia octandra and Osbeckia aspera in liver dysfunction in rats. *Ceylon J Med Sci*. 1999;42(1):1. doi:10.4038/cjms.v42i1.4882

49. Thabrew MI, Gove CD, Hughes RD, McFarlane IG, Williams R. Protective effects of Osbeckia octandra against galactosamine and tert-butyl hydroperoxide induced hepatocyte damage. *J Ethnopharmacol*. 1995;49(2):69-76. doi:10.1016/0378-8741(95)90033-0

50. Thabrew M., Hughes R., Gove C., Portmann B, Williams R, McFarlane I. Protective effect of Osbeckia octandra against paracetamol-induced liver injury. *XENOBIOTICA*. 1995;25(9):1009-1017.

51. Blanquicett C, Johnson MR, Heslin M, Diasio RB. Housekeeping gene variability in normal and carcinomatous colorectal and liver tissues: Applications in pharmacogenomic gene expression studies. *Anal Biochem*. 2002;303(2):209-214. doi:10.1006/abio.2001.5570

52. Lardizábal MN, Nocito AL, Daniele SM, Ornella LA, Palatnik JF, Veggi LM. Reference Genes for Real-Time PCR Quantification of MicroRNAs and Messenger RNAs in Rat Models of Hepatotoxicity. *PLoS One*. 2012;7(5):e36323. doi:10.1371/journal.pone.0036323

53. Ooki T, Hatakeyama M. Protocol for visualizing conditional interaction between transmembrane and cytoplasmic proteins. *STAR Protoc*. 2021;2(2):100430. doi:10.1016/j.xpro.2021.100430

54. Singh A, Bajpai V, Kumar S, Sharma KR, Kumar B. Profiling of gallic and ellagic acid

derivatives in different plant parts of Terminalia arjuna by HPLC-ESI-QTOF-MS/MS. *Nat Prod Commun*. 2016;11(2):239-244. doi:10.1177/1934578x1601100227

55. Yamanaka F, Hatano T, Ito H, Taniguchi S, Takahashi E, Okamoto K. Antibacterial Effects of Guava Tannins and Related Polyphenols on Vibrio and Aeromonas Species. *Nat Prod Commun*. 2008;3(5):711-720. doi:10.1177/1934578X0800300509

56. Haikal A, El-Neketi M, Elshaer S, Gohar AA, Hassan MA. Mentha longifolia subsp. typhoides and subsp. schimperi: Antimicrobial and Antiquorum-Sensing Bioactivities. *Chem Nat Compd*. 2021;57(5):933-938. doi:10.1007/s10600-021-03516-6

57. Varga J, Pasche B. Antitransforming growth factor-β therapy in fibrosis: recent progress and implications for systemic sclerosis. *Curr Opin Rheumatol*. 2008;20(6):720-728. doi:10.1097/BOR.0b013e32830e48e8

58. Kamm DR, McCommis KS. Hepatic stellate cells in physiology and pathology. *J Physiol*. 2022;600(8):1825-1837. doi:10.1113/JP281061

59. Gutierrez-Ruiz MC, Gomez-Quiroz LE. Liver fibrosis: Searching for cell model answers. *Liver Int*. 2007;27(4):434-439. doi:10.1111/j.1478-3231.2007.01469.x

60. Hoffmann C, Djerir NEH, Danckaert A, et al. Hepatic stellate cell hypertrophy is associated with metabolic liver fibrosis. *Sci Rep*. 2020;10(1):1-13. doi:10.1038/s41598-020-60615-0

61. Shu Y, Liu X, Huang H, Wen Q, Shu J. Research progress of natural compounds in anti-liver fibrosis by affecting autophagy of hepatic stellate cells. *Mol Biol Rep*. 2021;48(2):1915-1924. doi:10.1007/s11033-021-06171-w

62. Xu L, Hui AY, Albanis E, et al. Human hepatic stellate cell lines, LX-1 and LX-2: New tools for analysis of hepatic fibrosis. *Gut*. 2005;54(1):142-151. doi:10.1136/gut.2004.042127

63. Schinagl M, Tomin T, Gindlhuber J, et al. Proteomic Changes of Activated Hepatic Stellate Cells. *Int J Mol Sci*. 2021;22(23):12782. doi:10.3390/ijms222312782

64. Senoo T, Sasaki R, Akazawa Y, et al. Geranylgeranylacetone attenuates fibrogenic activity and induces apoptosis in cultured human hepatic stellate cells and reduces liver fibrosis in carbon tetrachloride-treated mice. *BMC Gastroenterol*. 2018;18(1):1-7. doi:10.1186/s12876-018-0761-7

65. Landete JM. Ellagitannins, ellagic acid and their derived metabolites: A review about source, metabolism, functions and health. *Food Res Int*. 2011;44(5):1150-1160. doi:10.1016/j.foodres.2011.04.027

66. Lee GE, Kim RH, Lim T, et al. Optimization of accelerated solvent extraction of ellagitannins in black raspberry seeds using artificial neural network coupled with genetic algorithm. *Food Chem*. 2022;396(June):133712. doi:10.1016/j.foodchem.2022.133712

67. El-Lakkany NM, El-Maadawy WH, Seif el-Din SH, et al. Antifibrotic effects of gallic acid on hepatic stellate cells: In vitro and in vivo mechanistic study. *J Tradit Complement Med*. 2019;9(1):45-53. doi:10.1016/j.jtcme.2018.01.010

68. Goldsmith EC, Bradshaw AD, Spinale FG. Cellular Mechanisms of Tissue Fibrosis. 2. Contributory pathways leading to myocardial fibrosis: moving beyond collagen expression. *Am J Physiol Physiol*. 2013;304(5):C393-C402. doi:10.1152/ajpcell.00347.2012

69. Osawa Y, Kawai H, Tsunoda T, et al. Cluster of Differentiation 44 Promotes Liver Fibrosis and Serves as a Biomarker in Congestive Hepatopathy. *Hepatol Commun*. 2021;5(8):1437-1447. doi:10.1002/hep4.1721

70. Li W, Zhou C, Fu Y, et al. Targeted delivery of hyaluronic acid nanomicelles to hepatic

stellate cells in hepatic fibrosis rats. *Acta Pharm Sin B*. 2020;10(4):693-710. doi:10.1016/j.apsb.2019.07.003

71. Souchelnytskyi S, Rönnstrand L, Heldin CH, ten Dijke P. Phosphorylation of Smad signaling proteins by receptor serine/threonine kinases. *Methods Mol Biol*. 2001;124(3902421036):107-120. doi:10.1385/1-59259-059-4:107

72. Yan J, Hu B, Shi W, et al. Gli2 -regulated activation of hepatic stellate cells and liver fibrosis by TGF-β signaling. *Am J Physiol Liver Physiol*. 2021;320(5):G720-G728. doi:10.1152/ajpgi.00310.2020

73. Peng D, Fu M, Wang M, Wei Y, Wei X. Targeting TGF-β signal transduction for fibrosis and cancer therapy. *Mol Cancer*. 2022;21(1):1-20. doi:10.1186/s12943-022-01569-x

74. Yuan X, Gong Z, Wang B, et al. Astragaloside Inhibits Hepatic Fibrosis by Modulation of TGF- β 1/Smad Signaling Pathway. *Evidence-Based Complement Altern Med*. 2018;2018:1-13. doi:10.1155/2018/3231647

75. Duwaerts CC, Maiers JL. ER Disposal Pathways in Chronic Liver Disease: Protective, Pathogenic, and Potential Therapeutic Targets. *Front Mol Biosci*. 2022;8(January):1-21. doi:10.3389/fmolb.2021.804097

76. Hetz C, Chevet E, Harding HP. Targeting the unfolded protein response in disease. *Nat Rev Drug Discov*. 2013;12(9):703-719. doi:10.1038/nrd3976

77. Wang M, Wey S, Zhang Y, Ye R, Lee AS. Role of the unfolded protein response regulator GRP78/BiP in development, cancer, and neurological disorders. *Antioxidants Redox Signal*. 2009;11(9):2307-2316. doi:10.1089/ars.2009.2485

78. Wiseman RL, Mesgarzadeh JS, Hendershot LM. Reshaping endoplasmic reticulum quality control through the unfolded protein response. *Mol Cell*. 2022;82(8):1477-1491. doi:10.1016/j.molcel.2022.03.025

79. Luo D, Fan N, Zhang X, et al. Covalent inhibition of endoplasmic reticulum chaperone GRP78 disconnects the transduction of ER stress signals to inflammation and lipid accumulation in diet-induced obese mice. *Elife*. 2022;11:1-26. doi:10.7554/ELIFE.72182

80. Shi D, Jiang P. A Different Facet of p53 Function: Regulation of Immunity and Inflammation During Tumor Development. *Front Cell Dev Biol*. 2021;9(October):1-10. doi:10.3389/fcell.2021.762651

81. Wang L, Zhang Z, Li M, et al. P53-dependent induction of ferroptosis is required for artemether to alleviate carbon tetrachloride-induced liver fibrosis and hepatic stellate cell activation. *IUBMB Life*. 2019;71(1):45-56. doi:10.1002/iub.1895

82. Doumpas N, Lampart F, Robinson MD, et al. TCF / LEF dependent and independent transcriptional regulation of Wnt/β-catenin target genes . *EMBO J*. 2019;38(2):2009. doi:10.15252/embj.201798873

83. Lecarpentier Y, Schussler O, Hébert JL, Vallée A. Multiple Targets of the Canonical WNT/β-Catenin Signaling in Cancers. *Front Oncol*. 2019;9(November):1-17. doi:10.3389/fonc.2019.01248

84. Alfei S, Turrini F, Catena S, et al. Ellagic acid a multi-target bioactive compound for drug discovery in CNS? A narrative review. *Eur J Med Chem*. 2019;183:111724. doi:10.1016/j.ejmech.2019.111724